Analysis of Thermomagnetic Convection in a Vertical Layer of Ferromagnetic Fluid under Inclined Magnetic Field

by

Mst. Lovly Khatun

Roll No. 1551554

A dissertation for the confirmation of the degree of
Master of Science

Department of Mathematics
Khulna University of Engineering & Technology
Khulna-9203, Bangladesh

April 2017

Declaration

This is to certify that the thesis work entitled "Analysis of Thermomagnetic Convection in a Vertical Layer of Ferromagnetic Fluid under Inclined Magnetic Field" has been carried out by **Mst. Lovly Khatun** in the Department of Mathematics, Khulna University of Engineering & Technology, Khulna-9203, Bangladesh. The above mentioned thesis or any part of that has not been submitted elsewhere for the award of any degree or diploma.

Signature of Supervisor	Signature of Student
Dr. Md. Habibur Rahman	Mst. Lovly Khatun

Approval

This is to certify that the dissertation work entitled "Analysis of Thermomagnetic Convection in a Vertical Layer of Ferromagnetic Fluid under Inclined Magnetic Field" has been carried out by me under the supervision of Dr. Md. Habibur Rahman, Assistant Professor in the Department of Mathematics, Faculty of Civil Engineering, Khulna University of Engineering & Technology, Khulna-9203, Bangladesh. The above dissertation work or any part of this work has not been submitted anywhere for the award of any degree or diploma.

BOARD OF EXAMINERS

Mst. Lovly Khatun, 2017	Chairman, 2017

Dedication

This thesis is dedicated to my beloved parents, Md. Abdul Kader & Mst. Laizu Khatun and my sisters, Kamrunnahar Kamini & Samsunnahar Eity and to my brother, Rasel Ahmmed, those who have chosen underprivileged life to continue my smile.

Acknowledgements

First of all, I would like to bend myself to Almighty Allah for giving me the strength and confidence to complete my thesis work, successfully. It is a great pleasure to express my deepest gratitude and profound respect to my honourable supervisor, Dr. Md. Habibur Rahman, Assistant Professor in the Department of Mathematics at Khulna University of Engineering & Technology, who fully gave many invaluable advices, proper guidance, constant encouragement, constructive suggestions, understanding, and support to made it possible for me to work on a topic that was of great interest to me. This thesis could not have been completed without his generous and professional assistance. Especially, our meetings during the last couple of months were of great support. I am fortunate enough to complete my research work under his kind supervision. I enjoyed all our meetings and above all, want to thank him again for all the good advices.

I am also so much grateful to Prof. Dr. M. M. Touhid Hossain, the honourable Head, Department of Mathematics at Khulna University of Engineering & Technology, as well as the member of the oral examination committee, for his cordial advices to prepare my final thesis paper. It is also a great opportunity for me to show gratitude to my one of the most favourite teachers, Prof. Dr. Mohammad Arif Hossain, Department of Mathematics at Khulna University of Engineering & Technology, who contributed a lot to finish my work through sharing his efficient knowledge with me. I would like to thank Prof. Dr. Fouzia Rahman, Department of Mathematics at Khulna University of Engineering & Technology, who encouraged and supported me in every situation to accomplish my thesis work.

I would also like to thank all my teachers and research students of the Department of Mathematics at Khulna University of Engineering & Technology for their relentless en-

couragement in various ways throughout this work.

Finally, I want to give my gratitude to my family, particularly to my parents and my brother, without whom emotional and financial support the completion of my thesis would be merely impossible.

Mst. Lovly Khatun

Abstract

The main purpose of this study is to deal with the magneto-gravitational convection in a layer of ferromagnetic fluids between two vertical non-magnetic plates. One of the plates is kept at constant temperature. A uniform inclined external magnetic field under nonzero gravity conditions has been considered. In this research both the gravitational and magnetic effects are taken into account. Two distinct mechanisms, namely, thermogravitational(buoyancy-driven) and thermomagnetic, lead to the apprearance of various instability modes. The characteristics of all instability modes are investigated. The three types of instability patterns relating to thermogravitational, magnetic and magnetogravitational convection are found to exist in a normal magnetic field. The inclined external magnetic field conducts the preferential change of instability structures toward the hot wall, it induces an asymmetry with the problem, and then it brings qualitative change in the stability characteristics. It is found because of the angle of inclination of the magnetic field, where a preferred magnetic field is kept in an orientation angle that introduces maximum magneto-gravitational instability. The destabilizing effects due to thermal disturbances and the variation of fluid magnetization has been found in the flow domain. However, the related variation of a magnetic field can draw the energy from the perturbed flow field, which is depending on the orientation of the applied field thus playing a stabilizing role. The role of the buoyancy effects shifts from destabilizing in the gravity-dominated flow to stabilizing in flows with strong magnetic effects is also found.

Contents

List of Figures

List of Tables

Chapter 1

Introduction

1.1 Magnetic Fluids

Ferromagnetism is a solid state phenomena, and it happens at a high energy state (in other words, less preferred) of the material. When the material will melt then the molecules will rearrange themselves to a lower energy state and lose the magnetism. A magnet has magnetic domains aligned in a parallel fashion. This property is known as ferromagnetism. Ferromagnetism is the property of cobalt, nickel, iron, their alloys and some minerals that have these metals as compounds. The temperature at which certain materials lose their permanent magnetic properties, to be replaced by induced magnetism is called the Curie temperature or Curie point. The Curie temperature is named after Pierre Curie, who showed that magnetism of certain materials was lost at a critical temperature. As the temperature rises above a certain point then the atom vibrations cause a breakdown in this alignment and above the Curie temperature this alignment no longer exists. Thus the ferromagnetic material becomes a paramagnetic material above the Curie temperature.

Common non-conducting artificial magnetic fluids consist of magnetite colloids which contain ferro-magnetic (e.g. magnetite(Fe_3O_4)) nano-particles suspended in a carrier fluid, usually synthetic oil, water or kerosene. To prevent formation of magnetite aggregates and their subsequent sedimentation a surfactant such as oleic acid is frequently used. The industrial production of such fluids began in the 1960s. Now-a-days their manufac-

turing technology is significantly improved which enabled the range of ferrofluid applications to widen significantly. However due to the complexity of their composition physical properties of ferrofluids depend not only on the type of components used to make them, but also on the conditions of their storage and use and on the hydrodynamics of flows they are subject to introduction to thermomechanics of magnetic fluids, ferrohydrodynamics and magnetic fluids.

Understanding of these dependencies is currently far from being complete and will be subject of the proposed studies. Misleadingly made ferrofluids respond to an external magnetic field nearly to natural paramangnetic and diamagnetic fluids (i.e., water, protein solution, paramagnetic melts) and gases (i.e., oxygen). However the level of the polarization which can be accomplished in manufactured ferrofluids is many requests of extent higher than that in characteristic magnetic fluids. The magneto-thermal mechanism of convection allows the creation of a virtually arbitrary, controllable body force distribution not only in ferrofluid but also in diamagnetic and paramagnetic materials. A paramagnetic material can still be attracted by a magnetic field, but loses the ability to become a magnet itself. The Curie temperature has always been found to be lower than the melting point of a ferromagnetic material is non-magnetic.

In contrast to the melting point, magnetic fluids are multi-phase media containing solid magnetic particles that can be magnetized. Such suspensions can be used to transfer heat, and heat and mass transport in such liquid magnetics can be controlled by using an external magnetic field. The magnetic force is independent of gravity and its greatest utility will surely be in microgravity environments. For example crystal growth from protein and insulating paramagnetic melts. However, for usual diamagnetic and paramagnetic media, the pondermotive forces exerted by a typical magnet on the earth are insignificant compared to gravity-induced buoyancy ones. Thus, a magnetic fluid is very convenient liquid for ground-based modeling of magnetic-driven convection due to its superparamagnetic properties.

Artificial magnetic fluids, also known as ferrofluid. The term 'ferrofluid' is a portmanteau

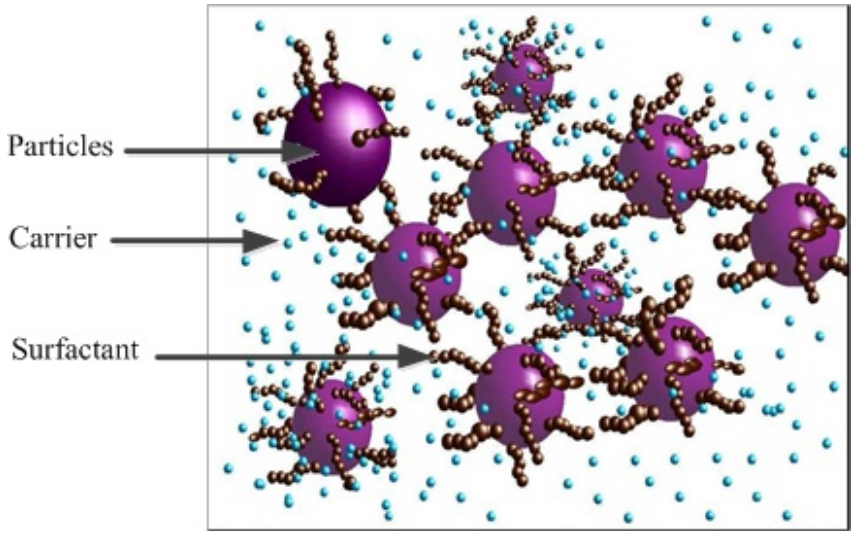

Figure 1.1: Surfacted ferrofluid (Tynjälä 2005). Used with permission.

of ferromagnetic and fluid and is used to describe a fluid that can be strongly magnetized by a magnetic field. This occurs because the fluid is composed of tiny magnetic particles, up to 100 times smaller than the wavelength of visible light. The most common minerals used in making these magnetic particles are iron oxides such as magnetite (Fe_3O_4) and hematite (Fe_2O_3), though other ferromagnetic or ferrimagnetic substances can be used.

The particles are usually less than 10 nm across. These tiny particles are suspended in a liquid carrier fluid, which can be water or an organic solvent. Thus, ferrofluids can be termed colloidal liquids, as they contain evenly dispersed microscopic particles in another substance. A typical ferromagnetic fluid can have up to 10% of magnetic solids and up to 10% of surfactant by volume (Odenbach 2002). Due to the demagnetization and the chemical adsorption impact at the boundary of the magnetic core, there is a layer of demagnetized magnetite of thickness $\sim$1 nm near the particle boundary.

As seen from Figure 1.1 each particle is coated with an appropriate surfactant and the resulting fluid is known as surfacted ferrofluid. Once a magnetic field is applied to a ferrofluid, the nanoparticles are attracted and pull the entire liquid towards the magnetic field. However, if exposed to a strong magnetic force, some of the nanoparticles can be ripped out from the carrier fluid, forming an incredibly fine dust. To stop the clumping of the nanoparticles via van der Waals forces, a surfactant (usually a hydrocarbon) coating is applied to the surface of each of the metallic particles, which overcomes the weak inter-

particle attraction. The particles suspended in a ferrofluid conform to Brownian motion, which means particle movement is generally random and the liquid will not settle under standard conditions.

However, when placed in a magnetic field, they orient along the applied field and the fluid becomes magnetized. The degree of magnetization depends on the applied field strength and the local temperature and concentration of magnetic particles. Magnetization is the measure of how much the magnetic field affects a magnetizable (fluid) medium. The ferrofluid magnetization, under the equilibrium assumption, is a function of magnetic field intensity vector, colloid density and dimensional temperature. The equilibrium magnetization model postulates that equilibrium is achieved by the re-orientation of elementary magnetic moments along the applied field direction.

As secondary effects such as the Lorentz force are neglected, analysis of transport phenomena involving ferrofluids is intricately linked with fluid magnetization. Magnetization also describes how a material responds to an applied magnetic field as well as the way the material changes the magnetic field, and can be used to calculate the forces that result from those interactions. It can be compared to electric polarization, which is the measure of the corresponding response of a material to an electric field in electrostatics. Physicists and engineers usually define magnetization as the quantity of magnetic moment per unit volume. It is represented by a pseudovector.

Led by the arising Kelvin force a magnetized fluid tends to flow toward regions of a stronger magnetic field. In this study it is assumed that the concentration of magnetic phase remains uniform and therefore the influence of only the thermal and magnetic fields on the flow structure will be studied. Thus the ferrofluid magnetization will be assumed to depend only on the magnitude of the applied magnetic field as well as on the fluid magnetic susceptibility, which is the ratio of the magnetization in fluid to strength of the applied magnetic field.

In light of that ferrofluids discovered many practical applications in electronic gadgets, vitality transformation gadgets, isolation of oil from water, scientific instrumentation, tun-

able optical channels and deformity identification sensors and in regions, for example, pharmaceutical, mechanical and aeronautic design, craftsmanship, and so forth. Ferrofluids are widely employed in industry. In medicine, ferrofluids are used as the contrast agents for magnetic resonance imaging and can be used for cancer detection.

1.2 Objective and Motivation

This study manages thermomagnetic convection in ferromagnetic fluids, which are likewise mentioned to as Ferro fluids or attractive fluids. The impacts of uniform warmth source and attractive field are considered. Over the couple of past decades, the utilizations of magnetic and electric fields in fluid flow control picked up an extensive consideration with prospects in these regions, for example, pharmaceutical, concoction designing, atomic combination, fast silent printing and so on. The primary area relevant to this review is Ferrohydrodynamics: the investigation of non-conducting smooth movements brought about by forces made by magnetic fields.

To comprehend the material science of a complex flow conduct of magnetic fluids, and furthermore to get an essential data for mechanical applications a precise review through an appropriate hypothesis is vital. Fluids utilized as a part of the majority of the mechanically critical applications are non-isothermal. That is the reason the investigation of convection and heat exchange is required. Since ferrofluids respond to both thermal and magnetic fields, their physical and mathematical description is a challenging task. The greater part of the accessible reviews identified with heat transfer and convection in fluids take after Newtonian description. Normally, an arrangement of constitutive conditions is utilized including a steady thickness statement.

The flow of ferromagnetic colloidal suspension of magnetic solid particles, for example, magnetite in a carrier liquid between two differentially heated plates set in a uniform outer magnetic field is considered. The instability patterns have been identified when the applied field is typical to the plates are found to comprise of stationary magneto convection rolls and spreading thermomagnetic or thermo gravitational waves (Suslov 2008).

Two distinct mechanisms, thermo gravitational and thermomagnetic, are in charge of the presence of these instability modes.

For the present study, it is considered a three dimensional geometry of a wide and tall vertical fluid layer cooled from one side, heated from the other and kept in a uniform oblique magnetic field at an arbitrary angle to the plates. Such an experimental design is convenient to reproduce cautiously and it allows one to concentrate on exploring the physical phenomenon leading to a nontrivial fluid motion without being embarrassed by boundary complications. The goal of this study is to analyze various convective instabilities in ferromagnetic fluids driven by buoyancy and ponderomotive magnetic forces in an inclined applied magnetic field. The physical way of the so-induced instability modes and their most prominent features will likewise be resolved to give direction to the future trial examination.

Chapter 2

Literature Review

Ferrofluid is a colloid in which nano sized ferromagnetic materials are suspended in a non-magnetic fluid. The studies of magnetic properties of such colloids have been conducted since 1930s (Elmore 1938) but they intensified noticeably in the 1960s and 1970s when the industrial production of magnetic fluids became possible (Bashtovoy & Vislovich 1988). Nowadays a large number of literatures exists on the properties of ferrofluids, for example, (Rosensweig 1979, 1985, Bashtovoy & Vislovich 1988, Blums et al. 1989, 1997) and references therein. In the absence of a magnetic field, the magnetic moments of individual particles in ferrofluids are randomly oriented so that the fluids have no net magnetization. Thus they are often categorized as superparamagnets rather than ferromagnets (Albrecht et al. 1997). However, when placed in a magnetic field, they orient along the applied field and the fluid becomes magnetized. The degree of magnetization depends on the applied field strength and the local temperature and concentration of magnetic particles. Led by the arising Kelvin force a magnetized fluid tends to flow toward regions of a stronger magnetic field. In this study it is assumed that the concentration of magnetic phase remains uniform and therefore the influence of only the thermal and magnetic fields on the flow structure will be studied. Such an assumption is reasonable if the characteristic timescale of convection flows of interest is much shorter than that of magnetic fluid segregation due to Soret effect or thermophoresis of solid particles (Shliomis & Smorodin 2002). Thus the ferrofluid magnetization will be assumed to depend only on

the magnitude of the applied magnetic field as well as on the fluid magnetic susceptibility, which is the ratio of the magnetization in fluid to strength of the applied magnetic field.

As ferrofluids are paramagnetic, they comply with Curie's law and accordingly turn out to be less charged at higher temperatures. Within the sight of temperature variety, magnetic buoyancy force is prompted in a ferrofluid which prompts to fluid motion known as convection. Convective heat transfer is one of the major types of heat transfer and convection is also a major mode of mass transfer in fluids. Convective heat and mass transfer take place both by diffusion. The relevent literature review follows three types of convective flows stated here.

Natural convection which can only occur in a gravitational field. A natural convection occurs because of temperature variations, which influence the fluids density and accordingly relative buoyancy of the fluid. Denser ingredients will fall while less dense ones will rise prompting to a bulk fluid motion. Gravitational convection is a type of natural convection induced by buoyancy variations resulting from material properties other than temperature. Gravitational convection also requires a g-force environment in order to occur. At the point when temperature sensitive ferrofluid experiences a temperature variety in the presence of an external magnetic field, a thermomagnetic force emerges, which drives more strenuous magnetized colder fluid particles to the areas with a stronger magnetic field. This phenomenon is known as magneto-convection and thermomagnetic convection the current study will be discussed focusing on.

Berkovskii & Bashtovoi (1971) examined the problem of gravitational convection for incompressible non-directing ferromagnetic fluid coming about because of the magnetocaloric impact. The natural convection is equal to this problem with a vertical temperature gradient. In their review, closed form solutions for both velocity and temperature are acquired and numerical calculations of the critical magnetic field gradients are given.

Established Rayleigh-Bénard convection (RBC) is brought about by the unsteadiness of a fluid layer. It is kept between two horizontal plates. And it is heated from below to propagate a fixed temperature distinction. In the standard Rayleigh-Bénard issue, the un-

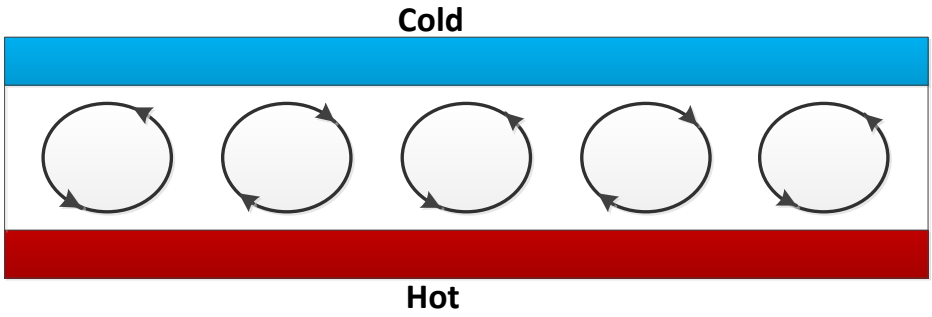

Figure 2.1: Cross-sectional schematic view of cell illustrating convection rolls.

steadiness of the fluid is driven by a density difference and brought about by a thermal expansion. In the fluid layer, the hot fluid at the base of the cell expands and propagates destabilizing density gradient, since fluids regularly have positive tharmal expansion coefficient. The hot fluid rises bringing about a convective flow which results in improved transport of heat between the two horizontal plates if the density gradient is sufficiently large.

There are two procedures that restrict fluids flow amplification. Firstly, viscous damping in the fluid directly restricts the fluid flow. Secondly, decreasing the buoyancy, thermal diffusion suppresses the temperature fluidity by making the temperature of the rising flame of hot fluid to balance with that of a surrounding fluid. If the flow amplifying effect exceeds the dissipative effects of thermal diffusion and buoyancy, the convection begins. The rotation of the cells interchanges from counter-clockwise to clock-wise as appeared in figure 2.1. If the temperature difference is vast, at that point the fluid rises rapidly, and a turbulent flow may happen. If the temperature difference is not far over the onset, the arising flow takes after upsetting of cylinders referred to as convection rolls.

Finlayson (1970) initially explained how an external uniform magnetic field connected to a ferrofluid with differing because of a temperature gradient magnetization comes about in a nonuniform magnetic body force, which leads to thermomagnetic convection. He examined theoretically the impact of a magnetic field connected vertically to an initially peaceful horizontal ferrofluid layer heated from below. He demonstrated that the magnetic mechanism dominates over the gravitational buoyancy mechanism in thin fluid layers that are about1 mm thick. The exact solution is obtained for some particular parameter values

and it is demonstrated that oscillatory instability can not happen when The fluid layers contained between two flat and free boundaries. Utilizing Galerkin technique approximate solutions for stationary instability are determined for two rigid boundaries(see additionally (Finlayson 1970, pp. 758 and 759)). Under certain conditions his examination predicted a solid coupling between the buoyancy and magnetic forces and demonstrated that the applied magnetic field can be used to control magnetic convection, which is important in ferrofluid innovation.

Schwab et al. (1983) performed an experiment to examine the influence of a homogeneous vertical magnetic field on the Bénard convection in a ferrofluid layer. The critical temperature difference was determined by measuring the effective thermal conductivity. The results agree with theoretical predictions.

Vaidyanathan et al. (1991) discussed the magnetoconvective instability in a ferromagnetic fluid using Brinkman model for saturated porous medium of very large permeability in a vertical magnetic field and showed that only stationary convection can occur. A linear convective instability analysis was performed accounting the critical temperature gradient when only the magnetic mechanism was important and when both buoyancy and magnetic mechanisms were present.

Siddheshwar (1995) concentrated a Convective instability of a ferromagnetic fluid in a Rayleigh-Bénard situation in a transverse uniform magnetic field between fluid-permeable, magnetic boundaries and subject to an external constraint. The fluid-permeable, magnetic boundaries require general boundary conditions on the velocity and the scalar magnetic potential. He utilized the Garlerkin method predicts the critical eigenvalue to be between that of free-free and rigid-rigid boundaries. The eigenvalue for stationary convection was gotten. The standard of trade of secure qualities was found to be substantial and oscillatory convection was discounted. The creator affirmed the subjective results of the past examination (Siddheshwar 1993) that were the constraining instance of his review.

Russell et al. (1995) investigated the heat transfer in strongly magnetized ferrofluids is calculated in the case where there was strong heating from above. The authors noticed

that the convection pattern at critical conditions has a large wave number, and this used to derive simplified equations for the temperature field in the ferrofluid. The results was found that the heat transfer depends non-linearly on the temperature difference.

Huang et al. (1997) performed the thermoconvective instability analysis of a laterally unbounded nonconducting horizontal layer of paramagnetic fluid heated from below subject to a uniform oblique magnetic field by using a linear stability analysis of the Navier-Stokes equations complemented with Maxwell's equations and accounting for the magnetic body force. The two-dimensional convective rolls with the axes parallel to the horizontal component of the magnetic field were shown to lead to the onset of convective instability.

Russell et al. (1999) analyzed the structure of two-dimensional vortices in a thin layer of a magnetized ferromagnetic fluid heated from above in the limit of large critical wavenumbers. They presented a nonlinear asymptotic description of the vortex pattern that occurs directly above the critical point in the parametric space where instability first sets in.

Lange et al. (2000) used linear stability theory to study the wavenumber selection of a free surface instability arising in a horizontal layer of viscous magnetic fluid of a finite depth in a normally applied magnetic field. The maximum growth rate and the corresponding wavenumber have been computed for various combinations of viscosity and thickness of a fluid layer. It has been found that the increase of magnetic induction leads to a mostly linear increase of a wavenumber, which is consistent with the experimental data. Another noteworthy results reported in Lange et al. (2000) is that in thin (film) layers of a fluid the behaviour of the disturbance wavenumber was found to be independent of the fluid viscosity and thus of the potential magnetoviscous effects.

Abraham (2002) analyzed the problem of Rayleigh-Bénard convection in a micropolar ferromagnetic fluid layer permeated by a uniform magnetic field analytically with free-free, isothermal, spin- vanishing, magnetic boundaries. The influence of the various micropolar and magnetization parameters on the threshold of stationary convection was discussed. It was found that micropolar fluid heated from below is more stable than ordinary

fluids. The nature of the magnetization effects on convection in a micropolar ferromagnetic fluid was found to be similar to that in Newtonian ferromagnetic fluids.

Suslov et al. (2008) investigated comprehensively a linear stability of convection flow in a layer of ferromagnetic fluid between two vertical differentially heated plates placed in a uniform external normal magnetic field. The author presented complete stability diagrams for two- and three-dimensional disturbances. It was found that two distinct mechanisms, thermogravitational and magnetic, are responsible for the appearance of three instability modes. The most prominent features were identified and the physical nature of all three modes was investigated in detail. The instability patterns were shown to depend on the governing parameters and to consist of vertical stationary magnetoconvection rolls and/or vertically or obliquely counterpropagating thermogravitational or thermomagnetic waves. It was also found that the growth rate of the stationary magnetoconvective instability is larger than that for the thermogravitational or thermomagnetic waves in a substantial part of a parametric space.

Belyaev & Smorodin (2010) studied by the Langevin law of magnetization the linear stability of a convective flow in a flat vertical layer of ferromagnetic fluid under a transverse temperature gradient in a uniform magnetic field perpendicular to the plates described. The stability of flow with respect to three-dimensional perturbations was analyzed, and the stability characteristics were obtained. The authors confirmed the existence of the stationary and two types of wave modes previously reported in Suslov et al. (2008). It was found that thermomagnetic waves can exist for a wide range of values of the magnetic susceptibility, Prandtl number and the Langevin parameter. The upper and lower boundaries of the interval of Prandtl numbers were determined where thermomagnetic waves with the large wavenumber found in Suslov et al. (2008) are generally unsafe.

Suslov et al. (2012) investigated theoretically and experimentally thermomagnetic convection flows patterns arising in a vertical differentially heated layer of nonconducting ferromagnetic fluid placed in an external uniform transverse magnetic field and discussed from the point of view of the perturbation energy balance. The authors investigated exper-

imentally various flow patterns and confirmed the existence of oblique thermomagnetic waves predicted by Suslov et al. (2008). It was shown that two distinct mechanisms, thermogravitational and magnetic, are responsible for the appearance of three instability modes. The physical nature of all three modes is investigated in detail and the most prominent features are identified to provide guidance for future experimental investigation. It was also found that the wavenumber of the detected convection patterns depends sensitively on the applied magnetic field and on the temperature difference across the layer. They suggested a quantitative criterion for detecting the parametric point where the dominant role in producing a flow instability is transferred between the thermomagnetic and thermogravitational mechanisms based on the disturbance energy balance analysis. It was found that such a transition occurs when Grashof and magnetic Grashof numbers are of comparable sizes.

Rahman & Suslov (2016) studied the fluids flow stability based on gravitational condition in a layer of ferrofluid confined between two vertical wide and tall non-magnetic plates. It heated from one side, cooled from the other and placed in a uniform oblique external magnetic field. There are two distinct mechanisms such as thermo-gravitational and thermo-magnetic, are found to be responsible for the appearance of various stationary and wave-like instability modes. The characteristics of all instability modes are investigated as functions of the orientation angles of the applied magnetic field and its magnitude for various values of magnetic parameters when both the thermo-magnetic and gravitational buoyancy mechanisms are active. The original three-dimensional instability patterns are recovered using the inverse Squire's transformation, and the optimal field and pattern orientations are determined.

In this study the major steps of the analyses reported in Finlayson (1970), Suslov (2008), Belyaev & Smorodin (2010), Suslov et al. (2012) and especially in Rahman & Suslov (2016) will be followed and focusing on the investigation of the influences of the orientation of the applied magnetic field on the fluid behaviour. Theoretically it will be clarified the observed ferrofluid motions on driving of the physical mechanisms. The fluids with weak (paramagnetic fluids) and strong (ferrofluids) degrees of magnetisation

will be obtained and the patterns resulting from the competition between thermomagnetic and thermograviational mechanisms of convection will be discussed for the comparative results. Further studies for this comprehensive investigation will also provide a guidance for future experiments.

Chapter 3

Problem Formulation and Governing Equations

In this chapter the geometry of the considered system along with the governing equations and their transformations will mainly be discussed.

3.1 Problem Formulation

Let us consider a ferromagnetic fluid that is flowing in between two infinitely extended vertical non-magnetic plates as shown in the figure 3.1. The origin of the right handed cartesian coordinate system (x, y, z) is placed at the middle of the plates such that the plates are at $x = \pm d$ and the gravity vector $\vec{\mathrm{g}}$ has the components $(0, -\mathrm{g}, 0)$. The plates are maintained at constant temperatures $T_* \pm \Theta$. An external uniform magnetic field with intensity $\vec{H}^e$ is applied with some inclinations to the plates. Let δ be the inclination angle with the x axis then $H_x^e = H^e \cos\delta$, and hence the component along the plates be $H^e \sin\delta$, thus $H_y^e = H^e \sin\delta \cos\gamma$ and $H_z^e = H^e \sin\delta \sin\gamma$, where γ is the angle made by the projection with the y axis. The applied magnetic field will create and induced magnetic field with strength $\vec{H}$ within the fluid i.e. there will be an induced magnetic field $\vec{H}$ having $|\vec{H}| = H$. The magnetic field causes fluid magnetization $\vec{M}$ such that $|\vec{M}| = M$, which is assumed to be co-directed with the internal magnetic field: $\vec{M} =$

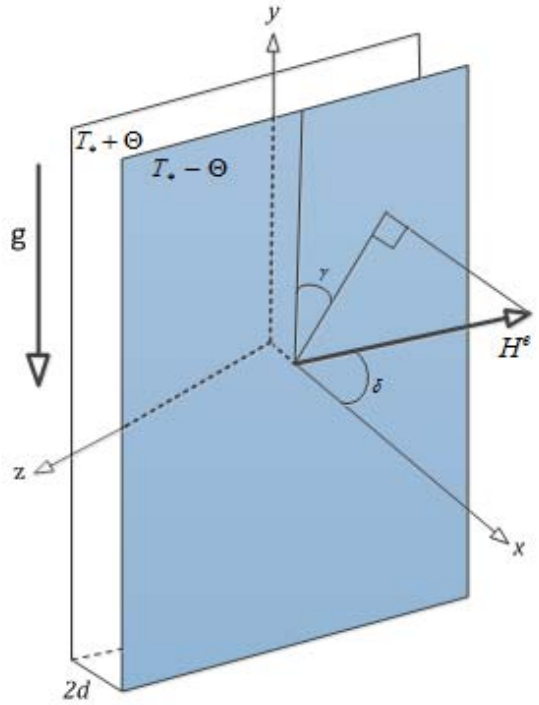

Figure 3.1: Sketch of the problem geometry.

$\chi_* \vec{H}$, where χ_* is the integral magnetic susceptibility of the fluid.

Assuming that the temperature difference 2Θ between the walls is sufficiently small we adopt the Boussinesq approximation to the continuity, Navier-Stokes and thermal energy equations that are complemented with the Maxwell equations for the magnetic field which is written in the magneto-static form due to the negligible electrical conductivity of ferrofluids (Rosensweig 1985). As discussed in Suslov (2008), the non-dimensional governing equations for velocity $\vec{v} = (u, v, w)$, temperature T, pressure p, magnetic field $\vec{H}$ and magnetization $\vec{M}$ written as

$$\nabla \cdot \vec{v} = 0\,, \tag{3.1.1}$$

$$\rho_* \frac{\partial \vec{v}}{\partial t} + \rho_* \vec{v} \cdot \nabla \vec{v} = -\nabla p + \eta_* \nabla^2 \vec{v} + \rho \vec{g} + \mu_0 M \nabla H\,, \tag{3.1.2}$$

$$\frac{\partial T}{\partial t} + \vec{v} \cdot \nabla T = \kappa_* \nabla^2 T\,, \tag{3.1.3}$$

$$\nabla \times \vec{H} = \vec{0}\,,\ \nabla \cdot \vec{B} = 0\,, \tag{3.1.4}$$

where

$$\vec{B} = \mu_0(\vec{M} + \vec{H}), \quad \vec{M} = \frac{M(H,T)}{H}\vec{H}. \tag{3.1.5}$$

where t is time, T is the temperature, p is the pressure, $\vec{B}$ is the magnetic flux density, ρ_* is the density, η_* is the dynamic viscosity, β_* is the coefficient of thermal expansion, κ_* is the thermal diffusivity, and $\mu_0 = 4\pi \times 10^{-7}$ H/m is the magnetic constant. The subscript $*$ denotes the values of the fluid properties evaluated at the reference temperature T_* and magnetic field $\vec{H}_*$. In writing equation (3.1.2) it is assumed that the fluid remains Newtonian. It has been found in experiments of Bogatyrev & Gilev (1984) that this is a reasonable approximation for fluids with the volume concentration of solid phase not exceeding $f = 0.1$.

The last term in equation (3.1.2) represents a ponderomotive (Kelvin) force that acts on a magnetized fluid in a nonuniform magnetic field driving it toward regions with a stronger magnetic field as discussed in Bashtovoy & Vislovich (1988). In order to close the problem, a magnetic equation of state is required which is assumed to be in the simplest linear form valid for small temperature and field variations within the layer,

$$M = M_* + \chi\Delta H - K\Delta T, \quad \Delta H \equiv H - H_*, \quad \Delta T \equiv T - T_*. \tag{3.1.6}$$

Here H_* and $M_* = \chi_* H_*$ are the magnitude of the magnetic field and the magnetisation at the location with temperature T_*, $\chi = \partial M/\partial H|_{(H_*,T_*)}$ is the differential magnetic susceptibility and $K = -\partial M/\partial T|_{(H_*,T_*)}$ is the pyromagnetic coefficient. Using equation (3.1.6), rewrite equation (3.1.5) as

$$\vec{M} = \frac{\chi H + (\chi_* - \chi)H_* - K\Delta T}{H}\vec{H}. \tag{3.1.7}$$

Equation (3.1.7) was used for computations reported in Rahman & Suslov (2015). However it leads to expressions that are algebraically quite involved. Therefore it is desirable

to use a simplified linearized version of equation (3.1.7), namely, its linearization

$$\vec{M} = [M_* + (\chi - \chi_*)\Delta H - K\Delta T]\vec{e}_* + \chi_*\Delta\vec{H}\,, \tag{3.1.8}$$

where $\vec{e}_* \equiv \vec{H}_*/H_* = (e_{1*}, e_{2*}, e_{3*})$, $\chi_* \equiv M_*/H_*$, $H = H_* + \Delta H$ and $\vec{H} = \vec{H}_* + \Delta\vec{H}$ so that $|\vec{H}_*| = H_*$ is the constant vector representing the major direction of the magnetic field and Δ denotes small increments. This was done previously in Finlayson (1970) and Suslov et al. (2008). Here the simplified equation (3.1.8) will also be used and the results will be compared with those reported in Rahman & Suslov (2015) for full equation (3.1.7).

Eliminating the magnetization in favor of the magnetic field one then obtains from the second of equations (3.1.4)

$$(1 + \chi_*)\nabla \cdot \vec{H} + (\chi - \chi_*)\nabla H \cdot \vec{e}_* - K\nabla T \cdot \vec{e}_* = 0\,. \tag{3.1.9}$$

This equation shows that thermomagnetic coupling occurs mostly when the magnetic field and the temperature gradient have components in the same direction.

It is convenient to redefine pressure p entering the momentum equation (3.1.2) so that it includes both a hydrostatic component and a potential of Kelvin force (detail can be found Odenbach (2002, pp. 86, 87)). In order to do this equation (3.1.6) is used to write

$$\begin{aligned} \mu_0 M\nabla H &= \mu_0[M_* + \chi\Delta H - K\Delta T]\nabla H \\ &= \mu_0\nabla[M_* H + \frac{1}{2}\chi\Delta H^2] - \mu_0 K\Delta T\nabla H\,. \end{aligned}$$

It will be demonstrated in perturbation energy balance that only the non-potential component

$$F_K = -\mu_0 K\Delta T\nabla H$$

of Kelvin force can lead to the destabilization of a static mechanical equilibrium and result

in magnetoconvection. Upon introducing the modified pressure

$$P = p - \mu_0 \left[M_* H + \frac{1}{2}\chi \Delta H^2 \right] , \tag{3.1.10}$$

The standard no-slip/no-penetration and thermal boundary conditions are imposed.

$$\vec{v} = \vec{0}\,, \quad \Delta T = \pm\Theta \text{ at } x = \mp d \tag{3.1.11}$$

for velocity and temperature, respectively. The magnetic boundary conditions are

$$(\vec{H}^e - \vec{H}) \times \vec{n} = \vec{0}\,,\ (\vec{B}^e - \vec{B}) \cdot \vec{n} = 0 \text{ at } x = \pm d\,, \tag{3.1.12}$$

where superscript e denotes fields outside the layer and $\vec{n} = (1,0,0)$ is the normal vector to the walls. Using equation (3.1.9) the second of the conditions in equation (3.1.12) is rewritten as

$$[\vec{H}^e - \{(1+\chi_*)H_* + (\chi - \chi_*)\Delta H \pm K\Theta\}\vec{e_*} - (1+\chi_*)\Delta\vec{H}] \cdot \vec{n} = 0 \text{ at } x = \pm d\,. \tag{3.1.13}$$

Consistent with the Boussinesq approximation valid for small differences between the walls the fluid density variation with temperature T is accounted for only in the buoyancy term in equation (3.1.2) as

$$\rho = \rho_*[1 - \beta_*(T - T_*)]\,, \tag{3.1.14}$$

where β_* is the coefficient of thermal expansion.

Pressure p entering the momentum equation (3.1.2) is redefined using the density equation (3.1.14) and the magnetisation equation (3.1.6) and noting that

$$\begin{aligned} \rho\vec{g} + \mu_0 M \nabla H &= \rho_*[1 - \beta_*\Delta T)]\vec{g} + \mu_0[M_* + \chi\Delta H - K\Delta T]\nabla H \\ &= \nabla\{\rho_*(\vec{r}\cdot\vec{g}) + \mu_0[M_* H + \frac{1}{2}\chi\Delta H^2]\} - (\rho_*\beta_*\vec{g} + \mu_0 K\nabla H)\Delta T\,, \end{aligned}$$

where $\vec{r} = (x, y, z)$ is the position vector. Equation (3.1.2) then becomes

$$\rho_* \frac{\partial \vec{v}}{\partial t} + \rho_* \vec{v} \cdot \nabla \vec{v} \;=\; -\nabla P + \eta_* \nabla^2 \vec{v} - \rho_* \beta_* \Delta T \vec{g} - \mu_0 K \Delta T \nabla H\,, \quad (3.1.15)$$

where the modified pressure $P = p - \rho_*(\vec{r} \cdot \vec{\mathrm{g}}) - \mu_0 \left[M_* H + \frac{1}{2}\chi \Delta H^2 \right]$. The governing equations and boundary conditions are nondimensionalised by using thermal velocity. However, in this chapter the nondimensionalisation is changed by introducing the viscous velocity, which is representative of non-zero base flow velocity. The other scales are changed consistently so that the governing equations and boundary conditions are nondimensionalised with the reference quantities for length, velocity, temperature and thermodynamic pressure using

$$(x, y, z) = d(x', y', z')\,,\ \vec{v} = \tfrac{\eta_*}{\rho_* d}\vec{v}'\,,\ t = \tfrac{\rho_* d^2}{\eta_*} t'\,,\ P = \tfrac{\eta_*^2}{\rho_* d^2} P'\,,$$
$$\Delta T = \Theta\theta'\,,\ \vec{\mathrm{g}} = \mathrm{g}\vec{e}_{\mathrm{g}}\,,\ \vec{H} = \tfrac{K\Theta}{1+\chi}\vec{H}'\,,\ \vec{M} = \tfrac{K\Theta}{1+\chi}\vec{M}'\,,$$

where ρ_* is the density and η_* is the dynamic viscosity at the reference temperature T_*, $\vec{e}_{\mathrm{g}} = (0, -1, 0)$ and d is the half-distance between the vertical walls. Then omitting primes for simplicity of notation, we will have

$$\nabla \cdot \vec{v} = 0\,, \quad (3.1.16)$$
$$\frac{\partial \vec{v}}{\partial t} + \vec{v} \cdot \nabla \vec{v} = -\nabla P + \nabla^2 \vec{v} - \mathrm{Gr}\theta \vec{e}_{\mathrm{g}} - \mathrm{Gr}_m \theta \nabla H\,, \quad (3.1.17)$$
$$\frac{\partial \theta}{\partial t} + \vec{v} \cdot \nabla \theta = \frac{1}{\mathrm{Pr}} \nabla^2 \theta\,, \quad (3.1.18)$$
$$\nabla \times \vec{H} = \vec{0}\,, \quad (3.1.19)$$
$$(1 + \chi_*) \nabla \cdot \vec{H} + (\chi - \chi_*) \nabla H \cdot \vec{e}_* - (1 + \chi) \nabla \theta \cdot \vec{e}_* = 0\,, \quad (3.1.20)$$
$$\vec{M} = [(\chi - \chi_*)(H - N) - (1 + \chi)\theta]\vec{e}_* + \chi_* \vec{H} \quad (3.1.21)$$

with the boundary conditions

$$[\vec{H}^e - \{(\chi - \chi_*)(H - N) \mp (1 + \chi)\}\vec{e}_* - (1 + \chi_*)\vec{H}] \cdot \vec{n} = 0\,, \quad (3.1.22)$$
$$\vec{v} = \vec{0}\,,\ \theta = \mp 1 \text{ at } x = \pm 1\,. \quad (3.1.23)$$

Table 3.1: The typical values of experimental parameters and properties of the ferrofluid manufactured in Scientific Laboratory of Practical Ferromagnetic Fluids, Ivanovo, Russia under Technical Conditions 229-001-02068195-2002 and used in experiments reported in Suslov et al. (2012) and Bozhko et al. (2013).

Notation	Parameter	Typical value
f	Volume concentration of magnetic phase	0.1
ρ_*	Density	1.44×10^3 kg/m^3
β_*	Coefficient of thermal expansion	7.7×10^{-4} K^{-1}
κ_*	Thermal diffusivity	1×10^{-8} m^2/s
η_*	Dynamic viscosity in the absence of magnetic field	7.66×10^{-3} kg/m s
K	Pyromagnetic coefficient	$\sim 10^2$ A/m K
μ_0	Magnetic constant	$4\pi \times 10^{-7}$ H/m
H^e	External magnetic field	$0 - 3.5 \times 10^4$ A/m
T_*	Average (reference) temperature in the layer	293 K
2Θ	Temperature difference between the walls	$1 - 30$ K
$2d$	Distance between the walls	6 mm

The rest of the governing equations and boundary conditions (3.1.16)-(3.1.23) remain unchanged. The new dimensionless parameters appearing in the problem are

$$\mathrm{Gr} = \frac{\rho_*^2 \beta_* \Theta g d^3}{\eta_*^2}, \quad \mathrm{Gr}_m = \frac{\rho_* \mu_0 K^2 \Theta^2 d^2}{\eta_*^2 (1+\chi)},$$
$$\mathrm{Pr} = \frac{\eta_*}{\rho_* \kappa_*}, \quad N = \frac{H_* (1+\chi)}{K\Theta}, \tag{3.1.24}$$

The thermal and magnetic Grashof numbers Gr and Gr_m characterise the importance of buoyancy and magnetic forces, respectively, the Prandtl number Pr is the ratio of viscous and thermal diffusion transports, and parameter N describes the strength of the magnetic field at the reference location relative to the variation of fluid magnetisation due to thermal effects. The values of Grashof numbers are chosen below to produce the complete parametric instability regions. The flow stabilization depends on the type of fluids characterized by viscosity and consequently fluids Prandtl number. We fix the value of Prandtl number to $\mathrm{Pr} = 27.5$ and choose $\chi = \chi_* = 3$ (which corresponds to a linear magnetisation regime) as in experiments of (Bozhko et al. 2013). In accordence with Rahman & Suslov (2015) we also have considered smaller values of $\chi = 1.5$ and 0.5 and of $\chi = 2.5$

and 1.5 that correspond to the near-saturation magnetic regimes.

Rahman & Suslov (2015) has characterized the thermo-magnetic sensitivity of thermo-fluids by the pyromagnetic coefficient K, which is related to the non-dimensional parameter N defined in equation (3.1.24) in which it has relation with the magnetic field H^e. As per definition more thermomagnetically sensitive fluids are characterized by the smaller values of N and H^e. Suslov et al. (2010, 2012), Bozhko et al. (2013) and Sidorov (2016) have considered the value of the non-dimensional external magnetic field H^e as 100 to compare the behaviour of fluids with different thermo-magnetic sensitivities. Where as Rahman & Suslov (2015) has chosen $H^e = 10$ to highlight the effects caused by the nonlinearity of magnetic field within the fluid layer.

In this investigation the inclination angle of the magnetic field is taken between 0 to 15° i.e $0^\circ \leq \delta \leq 15^\circ$ is considered. And the orientation has been considered between 0 to 180° i.e $0^\circ \leq \delta \leq 180^\circ$. It may be worthy to mention that the values of the Grashof numbers Gr and Gr_m were not restricted.

3.2 Basic flow and linearized perturbation equations

The steady solutions of equations (3.1.16)-(3.1.23) are in the form

$$\vec{v}_0 = (0, v_0(x), 0)\,,\ \theta_0 = \theta_0(x)\,,\ P_0 = P_0(x)\,,\ \vec{H}_0 = (H_{x0}(x), H_{y0}, H_{z0})\,.$$

They should satisfy

$$DP_0 = -\mathrm{Gr}_m \theta_0 e_{10} DH_{x0}\,,\ D^2 v_0 = -\mathrm{Gr}\theta_0\,,\ D^2\theta_0 = 0\,. \tag{3.2.1}$$

$$(1+\chi_*)DH_x 0 + (\chi - \chi_*)e_{10}e_{10*}DH_x 0 - (1+\chi)e_{10*}D\theta_0 = 0\,, \tag{3.2.2}$$

$$DH_{y0} = 0\,,\ DH_{z0} = 0\,, \tag{3.2.3}$$

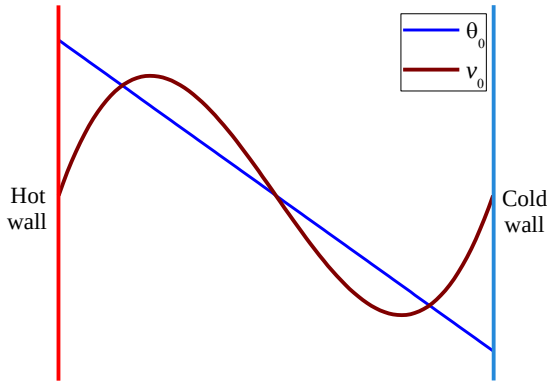

Figure 3.2: Pattern of basic convective flow.

and the boundary conditions

$$H_x^e - (\chi - \chi_*)(H_0 - N)e_{10*} \pm (1+\chi_*)e_{10*} - (1+\chi_*)H_{x0} = 0\,, \tag{3.2.4}$$

$$\theta_0 = \pm 1\,,\ H_{y0}(x) = H_y^e\,,\ H_{z0}(x) = H_z^e\,,\ \text{at } x = \mp 1\,. \tag{3.2.5}$$

where $H_0 \equiv \sqrt{H_{x0}^2 + H_{y0}^2 + H_{z0}^2}$, $M_0 \equiv \sqrt{M_{x0}^2 + M_{y0}^2 + M_{z0}^2}$ and $D \equiv \frac{d}{dx}$. Upon introducing the unit vector $\vec{e_0}(x) \equiv (e_{10}(x), e_{20}(x), e_{30}(x)) = \left(\frac{H_{x0}}{H_0}, \frac{H_y^e}{H_0}, \frac{H_z^e}{H_0}\right)$ in the direction of the magnetic field the basic flow solutions of equations (3.2.1) are written as

$$\theta_0 = -x\,,\ v_0 = \frac{\mathrm{Gr}}{6}(x^3 - x)\,,\ P_0 = \mathrm{Gr}_m \int \widetilde{x} e_{10} D H_{x0}\, \mathrm{d}\widetilde{x} + C\,, \tag{3.2.6}$$

where C is an arbitrary constant. Which is shown in figure 3.2. Equations (3.2.3) along with boundary conditions (3.2.5) result in the expressions for tangential components of the magnetic field that are constant inside the fluid layer $H_{y0}(x) = H_y^e$ and $H_{z0}(x) = H_z^e$. So the tangential components of the applied magnetic field do not change across the layer. It is informed (e.g. Suslov (2008)) that for a perpendicular field when $\vec{e} = \vec{e_*} = (1,0,0)$ the basic flow component of the magnetic field in the x direction across the layer is given by $H_{x0} = N_0 - x$, where N_0 is defined by $H^{e\prime} = (1+\chi_*)N_0$. But the nonlinear variation of an inclined magnetic field across the fluid layer cannot be given in a closed form and has to be computed numerically by solving the equation (3.2.2). When the field inclination angle is small i.e when $\sin\delta = \frac{\sqrt{H_y^2 + H_z^2}}{H^e} \to 0$, this solution can also be

written asymptotically as

$$\begin{aligned} H_{x0} = N_0 \;&-\; x + \frac{x(1+\chi_*)^2\sin^2\delta}{2(1+\chi)(N_0-x)}\left[(N_0-x)(1+\chi_*)+N_0(\chi_*-\chi)\right] \\ &-\; \frac{x(1+\chi_*)^4\sin^4\delta}{8(1+\chi)^2(N_0-x)^3}[(N_0-x)^3(1+\chi_*)(3+\chi+2\chi_*) \\ &+\; (N_0-x)N_0(\chi_*-\chi)(3+\chi+2\chi_*)(2N_0-x) \\ &+\; N_0^3(\chi_*-\chi)(1-\chi+2\chi_*)] + \circ((1+\chi_*)^4\sin^4\delta)\,, \end{aligned} \tag{3.2.7}$$

It can be also shown that for small non-zero inclination angles δ the nondimensional magnetic field at the center plane of a fluid layer is

$$N \approx N_0\sqrt{1+(1+\chi_*)^2\sin^2\delta}\,. \tag{3.2.8}$$

This approximation remains accurate as long as $(1+\chi_s)^2\sin^2\delta \ll 1$. For example, if $\chi_* = 5$ the above expression indicates that a significant change of the internal magnetic field value is expected to occur for the field inclination angles as small as $\delta = 10^\circ$. This is also evidenced by the numerical stability results that experience a qualitative change at similar inclinations. Then H_{x0} can be given in terms of $\frac{x}{N_0}$ as

$$\begin{aligned} \frac{H_{x0}}{N_0} = 1 - \frac{x}{N_0}\Big(1 &- \frac{1-\chi+2\chi_*}{2(1+\chi)}(1+\chi_*)^2\sin^2\delta \\ &- \frac{\chi^2-3+(3+2\chi_*)(2\chi-4\chi_*)}{8(1+\chi)^2}(1+\chi_*)^4\sin^4\delta\Big) \\ + \frac{x^2}{N_0^2}\frac{\chi_*-\chi}{2(1+\chi)}(1+\chi_*)^2\sin^2\delta &\left(1+3\frac{(1+\chi_*)^3}{1+\chi}sin^2\delta\right) \\ &+ \frac{x^3}{N_0^3}\frac{\chi_*-\chi}{2(1+\chi)}(1+\chi_*)^2\sin^2\delta \\ &\times\left(1+\frac{9-\chi+10\chi_*}{2(1+\chi)}(1+\chi_*)^2\sin^2\delta\right)+\cdots. \end{aligned} \tag{3.2.9}$$

where the asymptotic can be developed by considering $N_0 \gg x$. If the magnetisation law is linear, that is if $\chi = \chi_*$ then the equations (3.2.7) and (3.2.9) reduce to

$$\frac{H_{x0}}{N_0} = 1 - \frac{x}{N_0} + \frac{x}{2N_0}$$
$$(1+\chi_*)^2 \sin^2\delta \left[1 - \frac{3}{4}(1+\chi_*)^2 \sin^2\delta + \cdots\right] \tag{3.2.10}$$

In the following sections the physical features of instability patterns and the corresponding critical parameters will be presented for an inclined external magnetic field applied at arbitrary angles.

The nonlinearity of the function $H_{x0}(x)$ that occurs in ferrofluids with large magnetic susceptibilities has been shown to play a symmetry-breaking role, which in turn leads to significant qualitative and quantitative changes in stability characteristics of the considered flow. Rahman & Suslov (2015) have shown that within a ferrofluid layer the wave-like instability that do not exist in a normal field has link to the curvature of magnetic field lines. In this study, it has been tried to focus how a thermomagnetically induced symmetry breaking interacts due to the introduction of the preferred direction along the gravity vector.

To investigate a linear stability of the basic state with respect to infinitesimal y and z-periodic disturbances the perturbed quantities are written in a normal form

$$(\vec{v}, P, \theta, \vec{H}, H, \vec{M}, M) = (\vec{v_0}, P_0, \theta_0, \vec{H}_0, H_0, \vec{M}_0, M_0)$$
$$+ \left[(\vec{v_1}(x), P_1(x), \theta_1(x), \vec{H}_1(x), H_1(x), \vec{M}_1(x), M_1(x))e^{\sigma t + i(\alpha y + \beta z)} + c.c.\right] \tag{3.2.11}$$

where $\sigma = \sigma^R + i\sigma^I$ is the complex amplification rate, α and β are real wavenumbers in the y and z directions, respectively and c.c. denotes the complex conjugate of the expression in brackets. Upon introducing the magnetic potential $\phi_1(x)e^{\sigma t + i(\alpha y + \beta z)}$ of a

magnetic potential such that

$$\begin{aligned}
\vec{H}_1 &= [D\phi_1, i\alpha\phi_1, i\beta\phi_1]\,, \\
H_1 &= \vec{H}_1 \cdot \vec{e_0} = [e_{10}D + i(\alpha e_{20} + \beta e_{30})]\phi_1\,, \\
\vec{M}_1 &= [\chi_* D\phi_1 + e_{10*}(\chi - \chi_*)H_1 - e_{10*}(1+\chi)\theta_1\,, \\
&\quad i\alpha\chi_*\phi_1 + e_{20*}(\chi - \chi_*)H_1 - e_{20*}(1+\chi)\theta_1\,, \\
&\quad i\beta\chi_*\phi_1 + e_{30*}(\chi - \chi_*)H_1 - e_{30*}(1+\chi)\theta_1\,,]\,,
\end{aligned}$$

$$\begin{aligned}
M_1 &= \vec{M}_1 \cdot \vec{e_0} = [\chi_* + (\chi - \chi_*)(e_{10}e_{10*} + e_{20}e_{20*} + e_{30}e_{30*})]H_1 \\
&\quad -(1+\chi)(e_{10}e_{10*} + e_{20}e_{20*} + e_{30}e_{30*})\theta_1\,.
\end{aligned}$$

The linearization of equations (3.1.16)-(3.1.23) about the basic state leads to

$$Du_1 + i\,(\alpha v_1 + \beta w_1) = 0\,, \tag{3.2.12}$$

$$\begin{aligned}
\sigma u_1 &+ \left(\alpha^2 + \beta^2 + i\alpha v_0 - D^2\right) u_1 + DP_1 + e_{10}\mathrm{Gr}_m D H_{x0}\,\theta_1 \\
&+ \mathrm{Gr}_m\theta_0 e_{10} D^2\phi_1 + \mathrm{Gr}_m\theta_0\left(i(\alpha e_{20} + \beta e_{30}) + (1 - e_{10}^2)\frac{DH_{x0}}{H_0}\right) D\phi_1 \\
&- i\mathrm{Gr}_m\theta_0 e_{10}(\alpha e_{20} + \beta e_{30})\frac{DH_{x0}}{H_0}\phi_1 = 0\,,
\end{aligned} \tag{3.2.13}$$

$$\begin{aligned}
\sigma v_1 &+ Dv_0 u_1 + (\alpha^2 + \beta^2 + i\alpha v_0 - D^2)v_1 + i\alpha P_1 - \mathrm{Gr}\theta_1 \\
&+ i\alpha\mathrm{Gr}_m\theta_0 e_{10} D\phi_1 - \alpha\mathrm{Gr}_m\theta_0(\alpha e_{20} + \beta e_{30})\phi_1 = 0\,,
\end{aligned} \tag{3.2.14}$$

$$\begin{aligned}
\sigma w_1 \;&+\; (\alpha^2+\beta^2+i\alpha v_0 - D^2)w_1 + i\beta P_1 \\
&+\; i\beta \mathrm{Gr}_m \theta_0 e_{10} D\phi_1 - \beta \mathrm{Gr}_m \theta_0 (\alpha e_{20} + \beta e_{30})\phi_1 = 0\,, \qquad (3.2.15)\\
\sigma\theta_1 \;&\quad +D\theta_0 u_1 + \left(\frac{\alpha^2+\beta^2-D^2}{\mathrm{Pr}} + i\alpha v_0\right)\theta_1 = 0\,, \qquad (3.2.16)\\
&\quad (D^2-\alpha^2-\beta^2)\phi_1 - \frac{1+\chi}{1+\chi_*}[i(\alpha e_{20*}+\beta e_{30*}) + e_{10*}D]\theta_1 \\
&-\; \frac{\chi-\chi_*}{1+\chi_*}\left[(\alpha e_{20}+\beta e_{30})\left(\alpha e_{20*}+\beta e_{30*}+ie_{10}e_{10*}\frac{DH_{x0}}{H_0}\right)\phi_1 \qquad (3.2.17)\right.\\
&-\; \left(ie_{10}(\alpha e_{20*}+\beta e_{30*}) + ie_{10*}(\alpha e_{20}+\beta e_{30}) + e_{10*}(1-e_{10}^2)\frac{DH_{x0}}{H_0}\right)D\phi_1 \\
&-\; \left. e_{10}e_{10*}D^2\phi_1\right] = 0\,.
\end{aligned}$$

The disturbance velocity and temperature fields are subject to standard homogeneous boundary conditions

$$u_1 = v_1 = w_1 = \theta_1 = 0 \text{ at } x = \pm 1\,. \qquad (3.2.18)$$

For non-magnetic boundaries, a perturbation of a magnetic field within a fluid layer causes perturbation of the external magnetic field as observed in Finlayson (1970). If there are no induced currents outside the layer and a non-magnetic medium(air) fills the surrounding space, then the external magnetic field has a potential $\phi_1^e(x)exp(\sigma t + i\alpha y + i\beta z)$, which follows from equations (3.1.4) and (3.1.5), satisfies Laplace's equation

$$(D^2-\alpha^2-\beta^2)\phi_1^e = 0\,, \qquad (3.2.19)$$

in the regions $x < -1$ and $x > 1$. A physically relevant bounded solution can be written as

$$\phi_1^e(x) = Ae^{\sqrt{\alpha^2-\beta^2}x}\,,\ x < -1\,. \qquad (3.2.20)$$

and

$$\phi_1^e(x) = Be^{-\sqrt{\alpha^2-\beta^2}x}\,,\ x > 1\,. \qquad (3.2.21)$$

On considering the equation (3.1.5), the linearization of the magnetic boundary conditions

(3.1.12) leads to

$$D\phi_1^e = (1+\chi_*)D\phi_1 + e_{10*}(\chi-\chi_*)[i(\alpha e_{20}+\beta e_{30})+e_{10}D]\phi_1\,, \quad (3.2.22)$$

$$\phi_1^e = \phi_1 \quad \text{at} \quad x=\pm 1\,. \quad (3.2.23)$$

After eliminating A and B from equations (3.2.20), (3.2.21) and (3.2.23), the boundary conditions for ϕ_1 at $x=\pm 1$ becomes

$$(1+\chi_*)D\phi_1 \pm \sqrt{\alpha^2+\beta^2}\phi_1 + e_{10*}(\chi-\chi_*)[i(\alpha e_{20}+\beta e_{30})+e_{10}D]\phi_1 = 0\,. \quad (3.2.24)$$

Upon applying the generalized Squire's transformations

$$\begin{gathered}(x,y,z)=(\widetilde{x},\widetilde{y},\widetilde{z})\,,\ \theta_0=\widetilde{\theta}_0\,,\ H_{x0}=\widetilde{H}_{x0}\,,\ H_0=\widetilde{H}_0\,,\ \sigma=\widetilde{\sigma}\,,\ \alpha^2+\beta^2=\widetilde{\alpha}^2\,,\\ \beta=\widetilde{\beta}\,,\ u_1=\widetilde{u}\,,\ \alpha v_1+\beta w_1=\widetilde{\alpha}\widetilde{v}\,,\ w_1=\widetilde{w}\,,\ \theta_1=\widetilde{\theta}\,,\ P_1=\widetilde{P}\,,\ \phi_1=\widetilde{\phi}\,,\\ \alpha\mathrm{Gr}=\widetilde{\alpha}\widetilde{\mathrm{Gr}}\,,\ \mathrm{Gr}_m=\widetilde{\mathrm{Gr}}_m\,,\ \mathrm{Pr}=\widetilde{\mathrm{Pr}}\,,\ \chi=\widetilde{\chi}\,,\ \chi_*=\widetilde{\chi}_*\,, \quad (3.2.25)\\ e_{10*}=\widetilde{e}_{10*}\,,\ e_{10}=\widetilde{e}_{10}\,,\ \alpha e_{20}+\beta e_{30}=\widetilde{\alpha}\widetilde{e}_{20}\,,\ \alpha e_{20*}+\beta e_{30*}=\widetilde{\alpha}\widetilde{e}_{20*}\,,\end{gathered}$$

and noting that $\alpha v_0=\widetilde{\alpha}\widetilde{v}_0$, where $\widetilde{v}_0=\widetilde{\mathrm{Gr}}(\widetilde{x}^3-\widetilde{x})/6$, the equations (3.2.12)-(3.2.17)

become

$$D\widetilde{u} + i\widetilde{\alpha}\widetilde{v} = 0\,, \tag{3.2.26}$$

$$\begin{aligned}\widetilde{\sigma}\widetilde{u} \;&+\; (\widetilde{\alpha}^2 + i\widetilde{\alpha}\widetilde{v}_0 - D^2)\widetilde{u} + D\widetilde{P} + \widetilde{e}_{10}\widetilde{\mathrm{Gr}}_m D\widetilde{H}_{x0}\widetilde{\theta} + \widetilde{\mathrm{Gr}}_m\widetilde{\theta}_0\widetilde{e}_{10}D^2\widetilde{\phi} \\ &+\; \widetilde{\mathrm{Gr}}_m\widetilde{\theta}_0\left[i\widetilde{\alpha}\widetilde{e}_{20} + (1-\widetilde{e}_{10}^2)\frac{D\widetilde{H}_{x0}}{\widetilde{H}_0}\right]D\widetilde{\phi} - i\widetilde{\alpha}\widetilde{\mathrm{Gr}}_m\widetilde{\theta}_0\widetilde{e}_{10}\widetilde{e}_{20}\frac{D\widetilde{H}_{x0}}{\widetilde{H}_0}\widetilde{\phi} = 0\,,\end{aligned} \tag{3.2.27}$$

$$\begin{aligned}\widetilde{\sigma}\widetilde{v} \;&+\; D\widetilde{v}_0\widetilde{u} + (\widetilde{\alpha}^2 + i\widetilde{\alpha}\widetilde{v}_0 - D^2)\widetilde{v} + i\widetilde{\alpha}\widetilde{P} - \widetilde{\mathrm{Gr}}\widetilde{\theta} \\ &+\; \widetilde{\alpha}\widetilde{\mathrm{Gr}}_m\widetilde{\theta}_0(i\widetilde{e}_{10}D\widetilde{\phi} - \widetilde{\alpha}\widetilde{e}_{20}\widetilde{\phi}) = 0\,,\end{aligned} \tag{3.2.28}$$

$$\widetilde{\sigma}\widetilde{w} \;+\; (\widetilde{\alpha}^2 + i\widetilde{\alpha}\widetilde{v}_0 - D^2)\widetilde{w} + i\widetilde{\beta}\widetilde{P} + \widetilde{\beta}\widetilde{\mathrm{Gr}}_m\widetilde{\theta}_0(i\widetilde{e}_{10}D\widetilde{\phi} - \widetilde{\alpha}\widetilde{e}_{20}\widetilde{\phi}) = 0\,, \tag{3.2.29}$$

$$\widetilde{\sigma}\widetilde{\theta} \;+\; D\widetilde{\theta}_0\widetilde{u} + \left(\frac{\widetilde{\alpha}^2 - D^2}{\widetilde{\mathrm{Pr}}} + i\widetilde{\alpha}\widetilde{v}_0\right)\widetilde{\theta} = 0\,, \tag{3.2.30}$$

$$\begin{aligned}&(D^2 - \widetilde{\alpha}^2)\widetilde{\phi} - \frac{\widetilde{\chi} - \widetilde{\chi}_*}{1+\widetilde{\chi}_*}\widetilde{\alpha}\widetilde{e}_{20}\left[\widetilde{\alpha}\widetilde{e}_{20*} + i\widetilde{e}_{10*}\widetilde{e}_{10}\frac{D\widetilde{H}_{x0}}{\widetilde{H}_0}\right]\widetilde{\phi} \\ &+\; \frac{\widetilde{\chi} - \widetilde{\chi}_*}{1+\widetilde{\chi}_*}\left[i\widetilde{\alpha}(\widetilde{e}_{10}\widetilde{e}_{20*} + \widetilde{e}_{10*}\widetilde{e}_{20}) + \widetilde{e}_{10*}(1-\widetilde{e}_{10}^2)\frac{D\widetilde{H}_{x0}}{\widetilde{H}_0}\right]D\widetilde{\phi} \\ &+\; \frac{\widetilde{\chi} - \widetilde{\chi}_*}{1+\widetilde{\chi}_*}\widetilde{e}_{10*}\widetilde{e}_{10}D^2\widetilde{\phi} - \frac{1+\widetilde{\chi}}{1+\widetilde{\chi}_*}\left[i\widetilde{\alpha}\widetilde{e}_{20*} + \widetilde{e}_{10*}D\right]\widetilde{\theta} = 0\end{aligned} \tag{3.2.31}$$

with the boundary conditions

$$(1+\widetilde{\chi}_*)D\widetilde{\phi} \pm |\widetilde{\alpha}|\widetilde{\phi} + \widetilde{e}_{10*}(\widetilde{\chi} - \widetilde{\chi}_*)(i\widetilde{\alpha}\widetilde{e}_{20} + \widetilde{e}_{10}D)\widetilde{\phi} = 0\,, \tag{3.2.32}$$

$$\widetilde{u} = \widetilde{v} = \widetilde{w} = \widetilde{\theta} = 0 \quad \text{at} \quad \widetilde{x} = \pm 1\,. \tag{3.2.33}$$

Only (3.2.29) contains $\widetilde{w}$ and β explicitly. Therefore, this equation can be split from the rest of the transformed system and, if necessary, can be solved afterwards. By assuming the two-dimensionality of the perturbation field and its periodicity in the y direction can be formally obtained by setting $w = \beta = 0$, that the remaining equations form an equivalent two-dimensional problem. This enables one to significantly reduce the computational cost of stability calculations. However, even if β and w are set to 0 the external applied magnetic field $H_x^e = H^e\cos\delta$, $H_y^e = H^e\sin\delta\cos\gamma$ and $H_z^e = H^e\sin\delta\sin\gamma$ still remain three-dimensional in the above Squire-transformed linearised equations and thus the field inclination and orientation angles δ and γ still act as independent control parameters

entering the problem via the expressions for $\widetilde{e}_{10}$. The δ angle parameterizes the deviation of the field from the normal direction to the layer, while γ measures the azimuthal angle from the positive y direction that is from the direction opposite to that of the gravity. The equations have been solved by using numerical procedure and the obtained results have been plotted whenever deemed necessary.

Chapter 4

Results and Discussions

4.1 Comparison with Selected Previous Numerical Results

From the left plot of figure 4.1, it is evident that for each set of physical governing parameters, the problem is solved for a range of wave number $\widetilde{\alpha}$ to locate the maximum of the disturbance amplification rate $\widetilde{\sigma}^R$. Then the values of $\widetilde{\mathrm{Gr}}$ are iteratively modified until the maximum value of $\widetilde{\sigma}^R$ becomes smaller than the given threshold value of 10^{-5}. Full stability diagrams discussed in Section 4.2.3 are obtained by repeating the computational process for different values of $\widetilde{\mathrm{Gr}}_m$. The critical values of the governing parameters for the convection threshold in a perpendicular ($\delta = 0^\circ$) external magnetic field with magnitude H^e=100 have been computed to compare with previous results. For a pure gravitational convection ($\widetilde{\mathrm{Gr}}_m = 0$) threshold at Prandtl number $\widetilde{\mathrm{Pr}} = 0.71$, the critical values $\widetilde{\mathrm{Gr}} = 502.35$ and $\widetilde{\alpha} = 1.405$ are computed. After multiplying by the corresponding factors of 16 and 2, respectively, which is arising due to a different non-dimensionalisation they agree with the previously known accurate result reported in Suslov & Paolucci (1995). For $\widetilde{\mathrm{Pr}} = 7$, the onset of gravitational convection is also computed and the set of critical values $(\widetilde{\mathrm{Gr}}_m = 0, \widetilde{\mathrm{Gr}} = 491.78, \widetilde{\alpha} = 1.38)$ is obtained, which agree closely with those critical values presented in Belyaev & Smorodin (2010). The gravitational convection threshold is also computed for $\widetilde{\mathrm{Pr}} = 130$. The obtained critical

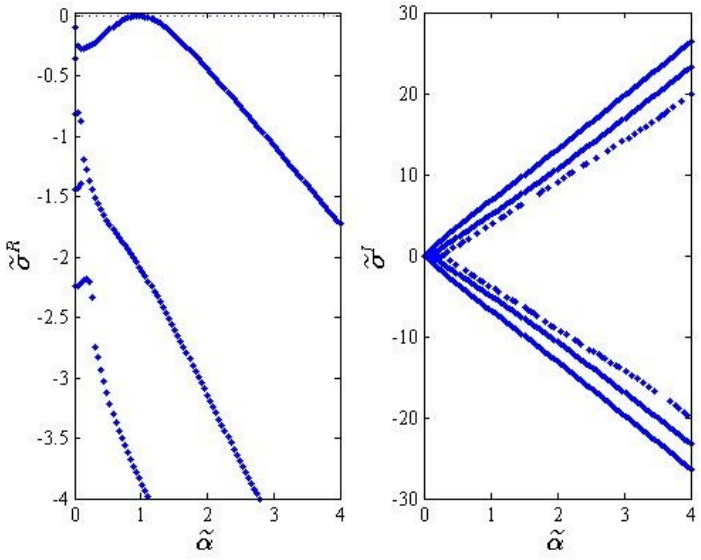

Figure 4.1: Leading disturbance temporal amplification rates $\widetilde{\sigma}^R$ (left) and frequencies $\widetilde{\sigma}^I$ (right) as functions of the combined wave number $\widetilde{\alpha}$ for $(\widetilde{\mathrm{Gr}}_m, \widetilde{\mathrm{Gr}}) = (0, 107.825)$ (onset of thermo-gravitational convection) at $\delta = \gamma = 0°$, $\widetilde{\chi} = \widetilde{\chi}_* = 5$ and $\widetilde{\mathrm{Pr}} = 27.5$.

values $\widetilde{\mathrm{Gr}} = 40.9735$ and $\widetilde{\alpha} = 1.2384$ are identical to those reported in Suslov et al. (2008). For the case of $\widetilde{\mathrm{Pr}} = 130$ and $\widetilde{\chi} = \widetilde{\chi}_* = 4$, the critical values for the magnetic convection threshold ($\widetilde{\mathrm{Gr}} = 0$) are computed and the critical values $\widetilde{\mathrm{Gr}}_m = 1.387$ and $\widetilde{\alpha} = 1.9278$ are obtained, which agree well with the values of $\widetilde{\mathrm{Gr}}_m = 1.385$ and $\widetilde{\alpha} = 1.95$ computed from the corresponding data reported in Finlayson (1970). For $\widetilde{\mathrm{Pr}} = 130$ and $\widetilde{\chi} = \widetilde{\chi}_* = 5$, the magnetic convection threshold is also determined and the critical values $\widetilde{\mathrm{Gr}}_m = 1.398$ and $\widetilde{\alpha} = 1.9366$ are obtained, which are identical to those reported in Suslov et al. (2008).

Moreover, for the case of Prandtl number $\widetilde{\mathrm{Pr}} = 130$ and $\widetilde{\chi} = \widetilde{\chi}_* = 5$, the critical values for mixed convection are computed. Two sets of critical values ($\widetilde{\mathrm{Gr}} = 16.69$, $\widetilde{\mathrm{Gr}}_m = 15.775$, $\widetilde{\alpha} = 1.6963$) and ($\widetilde{\mathrm{Gr}} = 39.976$, $\widetilde{\mathrm{Gr}}_m = 1.40$, $\widetilde{\alpha} = 1.2564$) are obtained, which agrees closely with those presented in Suslov et al. (2008).

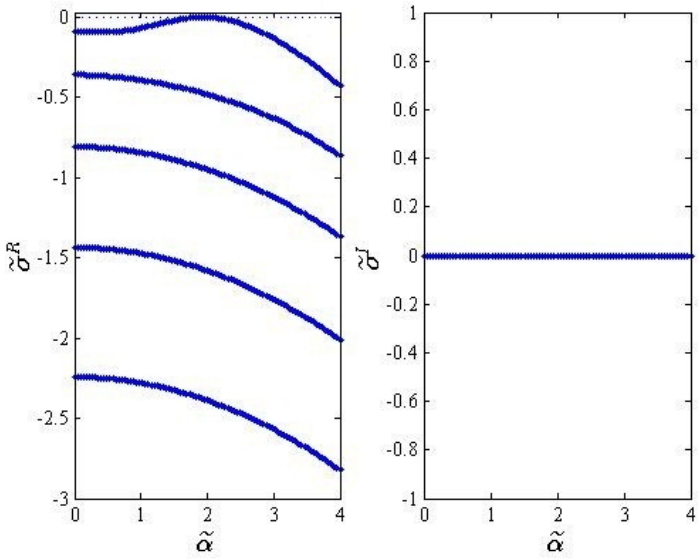

Figure 4.2: Same as Figure 4.1 but for $(\widetilde{\mathrm{Gr}}_m, \widetilde{\mathrm{Gr}}) = (6.609, 0)$ (onset of stationary magneto-convection).

4.2 Flow Stability Characteristics

4.2.1 Stability Characteristics of Flows in a Normal Field

Suslov (2008) has already investigated the stability characteristics of a ferromagnetic fluid flow in a vertical differentially heated layer placed in a normal magnetic field. Only flow stability in linearly magnetized fluid with the specific Prandtl number $\widetilde{\mathrm{Pr}} = 130$ has be discussed by the author. The present study contains the comprehensive stability characteristics of convection flow for different values of Prandtl number, arbitrary field inclination angles and both linear and non-linear magnetization of fluids.

In normal magnetic field, there exists three main types of instability patterns e.g. thermo-gravitational, magnetic and magneto-gravitational convections. The relevent typical eigen-value curves are shown in figures 4.1, 4.2 and 4.3 respectively.

From the figure 4.1, it is evident that, in the case of thermo-gravitational instability $(\widetilde{\mathrm{Gr}}_m \to 0)$ one maximum of the disturbance amplification rate $\widetilde{\sigma}^R$ exists with complex conjugate eigenvalues that indicate the existence of two counter-propagating waves. From the figure 4.2, it is also found that there is again maximum of the disturbance amplification rate $\widetilde{\sigma}^R$ but in this case $(\widetilde{\mathrm{Gr}} \to 0)$ the eigen-values are real and this situation corresponds

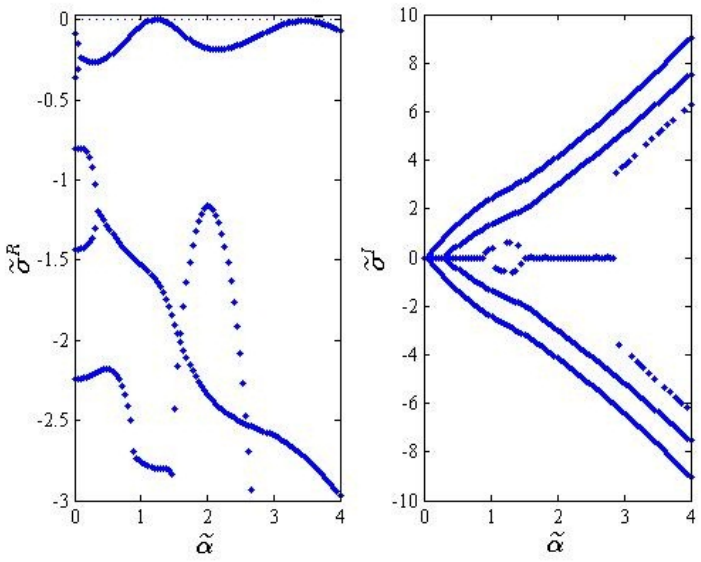

Figure 4.3: Same as Figure 4.1 but for $(\widetilde{\mathrm{Gr}}_m, \widetilde{\mathrm{Gr}}) = (124, 41.61)$. In the left plot the left and right maxima correspond to small- and large-wave number waves, respectively, and the middle maximum corresponds to a stationary roll pattern.

to a stationary magneto-convection pattern. In the third case ($\widetilde{\mathrm{Gr}} \neq 0, \widetilde{\mathrm{Gr}}_m \neq 0$) up to three maxima of the disturbance amplification rate $\widetilde{\sigma}^R$ (see figure 4.3) can exist, of which the left and right most maxima correspond to small and large-wave-number waves respectively while the middle one corresponds to a stationary magneto-convection pattern. These instability modes will be identified to as Type-I, III and II, respectively. It may be mentioned that the stabilities start with $\widetilde{\mathrm{Gr}} \neq 0, \widetilde{\mathrm{Gr}}_m = 0$; $\widetilde{\mathrm{Gr}} = 0, \widetilde{\mathrm{Gr}}_m \neq 0$ and $\widetilde{\mathrm{Gr}} \neq 0, \widetilde{\mathrm{Gr}}_m \neq 0$ are commonly characterized as thermo-gravitational, magnetic and magneto-gravitational convection respectively.

Rahman & Suslov (2016) have worked with the critical values of magnetic Grashof number, $\widetilde{\mathrm{Gr}}_m$ as 0, 12 and 30. They have found that for low values of $\widetilde{\mathrm{Gr}}_{mc}$, the wave number $\widetilde{\alpha}_c$ increases with the increase of Prandtl number $\widetilde{\mathrm{Pr}}$. But for high values $\widetilde{\mathrm{Gr}}_{mc}$, $\widetilde{\alpha}_c$ primarily increases and after achieving a maximum it decreases with the increase of Prandtl number $\widetilde{\mathrm{Pr}}$. In this research we have considered $\widetilde{\mathrm{Gr}}_{mc}$ as 5 and 10 as low values and 35 as high value and the same feature observed as reported in Rahman & Suslov (2016) (see Table 4.1) i.e., in case of low $\widetilde{\mathrm{Gr}}_{mc}$, $\widetilde{\alpha}_c$ increases but for high values it primarily increases and attaining to a maximum then it decreases with the increase of Prandtl number $\widetilde{\mathrm{Pr}}$.

In case of $\widetilde{\mathrm{Gr}}_c = 0$ i.e. in absence of buoyancy force with the increase of Prandtl number $\widetilde{\mathrm{Pr}}$ the critical value of magnetic Grashof number $\widetilde{\mathrm{Gr}}_{mc}$ decreases and $\widetilde{\alpha}_c$ remains constant. In other words the onset of a stationary magneto-convection (for $\widetilde{\mathrm{Gr}} = 0$) occurs at wave number that is independent of the values of Prandtl number $\widetilde{\mathrm{Pr}}$. The data in the Table 4.1 also confirms that the stationary magneto-convection pattern is characterized by the magnetic Grashof number $\widetilde{\mathrm{Gr}}_m$ that is inversely proportional to $\widetilde{\mathrm{Pr}}$. It may be noted that the disturbance wave speed of gravitational instability modes becomes larger than the maximum basic flow velocity in a large Prandtl-number fluid meaning that the physical nature of instabilities has nothing to do with the basic flow velocity field. It is also observed that the basic flow becomes less stable when Prandtl number increases. As Prandtl number is the ratio of fluids viscosity and thermal diffusivity, the large Prandtl number corresponds to small thermal diffusion. Therefore thermal disturbances dissipate slowly in large Prandtl-number fluids. Thus based on the data presented in Table 4.1, it may be concluded that the physical nature of instabilities observed for $\widetilde{\mathrm{Gr}}_m = 0$ is thermally dominated and because of that Gershuni and his colleagues called these waves as thermal (Gershuni et al. 1989). Thermal waves propagate to upwards near the hot wall and to downwards near the cold wall(see in Table 4.2). This conclusion remains mostly true for magneto-gravitational convection when both $\widetilde{\mathrm{Gr}}$ and $\widetilde{\mathrm{Gr}}_m$ are non-zero.

In a normal magnetic field, the representative critical values of $\widetilde{\mathrm{Gr}}$, $\widetilde{\alpha}$ and disturbance wave speed $\widetilde{c}$ for two thermomagnetic waves at $\widetilde{\mathrm{Gr}}_m = 12$ and $\widetilde{\mathrm{Pr}} = 27.5$ are given in Table 4.2 for various values of magnetic susceptibilities $\widetilde{\chi}$ and $\widetilde{\chi}_*$. In the case of linear magnetization law i.e. when $\widetilde{\chi} = \widetilde{\chi}_*$ the two waves propagate with equal speeds in the opposite directions. By the same wave number, the disturbance waves are characterized and the basic flow becomes unstable with respect to the first and second waves simultaneously propagating to upwards and downwards respectively.

However, when the values of $\widetilde{\chi}$ and $\widetilde{\chi}_*$ differ i.e. in the case of non-linear magnetization law close to the magnetic saturation the symmetry of wave is broken and the first wave near the hot wall becomes more dangerous compared to the second wave near the cold wall (see Table 4.2). By a slightly larger wave number the first wave is characterized than

Table 4.1: The critical values of $\widetilde{\mathrm{Gr}}_m$, $\widetilde{\mathrm{Gr}}$, $\widetilde{\alpha}$, disturbance wave speed $\widetilde{c} = -\widetilde{\sigma}^I/\widetilde{\alpha}$ and the maximum speed of the basic flow $\widetilde{v}_{0\,max}$ for mixed convection in a perpendicular ($\delta = 0^\circ$) external magnetic field $H^e = 100$ at $\widetilde{\chi} = \widetilde{\chi}_* = 5$ and various values of Prandtl number $\widetilde{\mathrm{Pr}}$.

$\widetilde{\mathrm{Pr}}$	$\widetilde{\mathrm{Gr}}_{mc}$	$\widetilde{\mathrm{Gr}}_c$	$\widetilde{\alpha}_c$	$\widetilde{c}_c$	$\widetilde{v}_{0\,max}$
20	5	149.980	0.824	±9.232	9.616
27.5	5	106.487	0.969	±6.662	6.828
55	5	62.979	1.153	±4.040	4.038
70	5	54.044	1.200	±3.489	3.465
130	5	37.108	1.308	±2.423	2.379
150	5	33.967	1.333	±2.222	2.178
20	10	149.083	0.828	±9.172	9.559
27.5	10	105.109	0.978	±6.568	6.739
55	10	60.389	1.183	±3.862	3.872
70	10	50.931	1.241	±3.274	3.266
130	10	31.987	1.401	±2.070	2.051
150	10	28.063	1.447	±1.815	1.799
20	35	144.378	0.845	±8.855	9.257
27.5	35	97.399	1.025	±6.043	6.245
55	35	38.291	1.459	±2.354	2.455
60	35	23.748	1.651	±1.395	1.523
65	35	11.036	1.498	±0.535	0.708
70	35	8.733	1.350	±0.382	0.560
75	35	7.071	1.234	±0.269	0.453
20	9.087	0	1.936	0	0
27.5	6.609	0	1.936	0	0
55	3.305	0	1.936	0	0
70	2.596	0	1.936	0	0
130	1.398	0	1.936	0	0
150	1.212	0	1.936	0	0

that of a second wave.

4.2.2 Wave-like Instabilities in Oblique Fields

Tables 4.3 and Tables 4.4 represent the similar critical values of $\widetilde{\mathrm{Gr}}$, $\widetilde{\alpha}$ and $\widetilde{c}$ for the first and second waves respectively of mixed convection at $\widetilde{\mathrm{Gr}}_m = 12$, $\gamma = 0^\circ$, $\widetilde{\mathrm{Pr}} = 27.5$, $H^e = 100$ (odd-numbered lines), $H^e = 10$ (even-numbered lines), and various values of

Table 4.2: The critical values of $\widetilde{\mathrm{Gr}}$, $\widetilde{\alpha}$ and disturbance wave speed $\widetilde{c} = -\widetilde{\sigma}^I/\widetilde{\alpha}$ for leading two waves of mixed convection in a normal magnetic field($\delta = 0°$) for $\widetilde{\mathrm{Gr}}_m = 12$, $\gamma = 0°$, $\widetilde{\mathrm{Pr}} = 27.5$, $H^e = 100$ and various values of $\widetilde{\chi}$ and $\widetilde{\chi}_*$.

		Upward propagating wave			Downward propagating wave		
$\widetilde{\chi}$	$\widetilde{\chi}_*$	$\widetilde{\alpha}_c$	$\widetilde{\mathrm{Gr}}_c$	$\widetilde{c}_c$	$\widetilde{\alpha}_c$	$\widetilde{\mathrm{Gr}}_c$	$\widetilde{c}_c$
5	5	0.981	104.54	6.530	0.981	104.54	-6.530
3	5	0.979	105.43	6.582	0.976	106.07	-6.623
3	3	0.982	104.25	6.510	0.982	104.25	-6.510
1.5	2.5	0.984	104.19	6.502	0.981	104.73	-6.538
1	2	0.982	104.47	6.519	0.978	105.36	-6.577
0.5	1.5	0.977	105.77	6.599	0.968	107.64	-6.720

$\widetilde{\chi}$ and $\widetilde{\chi}_*$. In those tables the critical values have been plotted for different values of δ for $\widetilde{\chi}$ and $\widetilde{\chi}_*$. As follows data in the Tables 4.3 and 4.4 the basic follow becomes more stable with the increases of the field inclination angles. The wave number of disturbance waves decreases with the increases of the field inclination angles and consequently, the distance between two instability rolls becomes longer. By the increases of the field inclination angles the disturbance waves propagate quicker.

The inclined magnetic field leads to the asymmetry in wave propagation compared to the normal field regardless of fluid magnetization is linear or not in the flow domain presented in the Tables 4.3 and 4.4. It is seen that the upward propagating wave for various inclined magnetic fields are always characterized by larger wave number than that of the downward propagating wave. The basic flow is less stable for the upward propagating wave compared to the downward propagating wave in the case of linear magnetization law. Consequent, the upward propagating waves remain the most dangerous in inclined magnetic fields. The upward wave propagates slowly compared to the downward wave. However, the destabilizing characters of the upward and downward waves swap near the magnetization saturation in the case of non-linear magnetization law. Thus, generally it is concluded that the strength of the applied arbitrary oblique magnetic field can charge quantitatively the stability characteristics.

It is noted that the equation (3.1.24) represents the magnitude of the non-dimensional

Table 4.3: The critical values of $\widetilde{\mathrm{Gr}}$, $\widetilde{\alpha}$ and disturbance wave speed $\widetilde{c} = -\widetilde{\sigma}^I/\widetilde{\alpha}$ for first wave of mixed convection at $\widetilde{\mathrm{Gr}}_m = 12$, $\gamma = 0^\circ$, $\widetilde{\mathrm{Pr}} = 27.5$, $H^e = 100$ (odd-numbered lines), $H^e = 10$ (even-numbered lines), and various values of $\widetilde{\chi}$ and $\widetilde{\chi}_*$.

		$\delta = 5^\circ$			$\delta = 10^\circ$			$\delta = 15^\circ$		
$\widetilde{\chi}$	$\widetilde{\chi}_*$	$\widetilde{\alpha}_c$	$\widetilde{\mathrm{Gr}}_c$	$\widetilde{c}_c$	$\widetilde{\alpha}_c$	$\widetilde{\mathrm{Gr}}_c$	$\widetilde{c}_c$	$\widetilde{\alpha}_c$	$\widetilde{\mathrm{Gr}}_c$	$\widetilde{c}_c$
5	5	0.989	104.50	6.539	0.976	107.38	6.734	0.964	109.64	6.885
		0.993	103.98	6.506	0.979	106.90	6.704	0.966	109.38	6.868
3	5	0.990	104.93	6.575	0.975	108.08	6.790	0.963	110.23	6.932
		0.992	105.05	6.578	0.973	108.23	6.801	0.962	110.24	6.933
3	3	0.991	103.61	6.476	0.986	105.12	6.583	0.976	107.12	6.718
		0.993	103.34	6.459	0.989	104.74	6.558	0.978	106.81	6.697
1.5	2.5	0.994	103.27	6.453	0.987	104.91	6.573	0.978	106.87	6.706
		0.995	103.07	6.441	0.990	104.69	6.555	0.980	106.87	6.702
1	2	0.994	103.24	6.450	0.990	104.37	6.538	0.983	106.04	6.653
		0.995	103.12	6.442	0.993	104.27	6.527	0.981	106.18	6.662
0.5	1.5	0.992	103.80	6.485	0.993	104.09	6.524	0.989	105.13	6.600
		0.993	103.77	6.483	0.992	104.06	6.524	0.989	105.09	6.598

magnetic field is proportional to parameter N, which is reciprocally proportional to the pyromagnetic coefficient that characterizes the sensitivity of the fluid magnetization to the temperature variation. The weaker temperature dependence fluids magnetization characterized by the large value of non-dimensional magnetic field and vice versa. It is concluded that the strength of the external stronger and weaker magnetic field corresponds to thermo-magnetically less and more sensitive fluids. From the Tables 4.3 and 4.4 it has been found that when an oblique magnetic field is applied the upward propagating wave in a thermo-magnetically more sensitive fluid is characterized by a larger wave number and the basic flow becomes less stable there than in a thermo-magnetically less sensitive fluid regardless of whether the fluid magnetization is linear or not. It has been also seen that whatever the fluid magnetization law is, the upward disturbance wave in a less thermo-magnetically sensitive fluid propagates quicker than that in a more thermo-magnetically sensitive fluid. Where as, in the case of the downward propagating wave in more thermo-magnetically sensitive fluid is characterized by a smaller wave number compared to that in a less thermo-magnetically sensitive fluid in an arbitrarily inclined magnetic field regardless of whether the fluid magnetization is linear or not. The basic

Table 4.4: Same as Table 4.3 but for second wave.

		$\delta = 5^\circ$			$\delta = 10^\circ$			$\delta = 15^\circ$		
$\widetilde{\chi}$	$\widetilde{\chi}_*$	$\widetilde{\alpha}_c$	$\widetilde{\mathrm{Gr}}_c$	$\widetilde{c}_c$	$\widetilde{\alpha}_c$	$\widetilde{\mathrm{Gr}}_c$	$\widetilde{c}_c$	$\widetilde{\alpha}_c$	$\widetilde{\mathrm{Gr}}_c$	$\widetilde{c}_c$
5	5	0.987	104.64	-6.548	0.975	107.49	-6.742	0.963	109.70	-6.889
		0.981	105.42	-6.597	0.970	108.04	-6.777	0.961	109.97	-6.906
3	5	0.989	105.44	-6.603	0.971	109.04	-6.845	0.959	111.14	-6.984
		0.985	105.39	-6.606	0.973	108.87	-6.834	0.960	111.12	-6.982
3	3	0.990	103.68	-6.481	0.985	105.22	-6.589	0.975	107.20	-6.723
		0.988	104.04	-6.504	0.981	105.69	-6.619	0.973	107.55	-6.745
1.5	2.5	0.992	103.48	-6.469	0.988	104.95	-6.572	0.978	107.04	-6.714
		0.990	103.72	-6.484	0.985	105.22	-6.592	0.976	107.06	-6.718
1	2	0.992	103.59	-6.475	0.991	104.46	-6.539	0.982	106.37	-6.669
		0.990	103.70	-6.483	0.988	104.57	-6.551	0.983	106.25	-6.661
0.5	1.5	0.988	104.52	-6.536	0.994	104.39	-6.535	0.987	106.05	-6.649
		0.988	104.45	-6.533	0.995	104.35	-6.532	0.987	106.05	-6.649

flow in a more thermo-magnetically sensitive fluid becomes more stable with respect to a downward propagating wave and its disturbance wave speed becomes quicker than those in a less thermo-magnetically sensitive fluid.

The figures 4.4, 4.5 and 4.6 represent the comparison among the critical parameter values of $\widetilde{\mathrm{Gr}}$, $\widetilde{\alpha}$ and $\widetilde{c}$ i.e., the flow stability characteristics as functions of the field inclination angle δ and orientation angle γ for $\widetilde{\mathrm{Gr}}_m = 12$, $H^e = 100$, $\widetilde{\mathrm{Pr}} = 27.5$ and the values of magnetic susceptibilities, $\widetilde{\chi} = \widetilde{\chi}_* = 3$, $\widetilde{\chi} = \widetilde{\chi}_* = 5$ and $\widetilde{\chi} = 1.5$, $\widetilde{\chi}_* = 2.5$, respectively. In the all figures the plots(a) describe the Grashof number $\widetilde{\mathrm{Gr}}$ (the flow is stable under the respective curves), (b) wave number $\widetilde{\alpha}$ and (c) wave speed $\widetilde{c}$ as functions of the inclination angle γ from 0 to 180°.

In the plot(a) in figure 4.4 the stability results are computed for a particular value of $\widetilde{\mathrm{Gr}}_m = 12$ to analyze the influence of the field orientation angle γ. Under the larger field inclination angles δ the basic flow becomes more stable regardless of the effect of field orientation angle γ. With the increase of the field inclination angle δ the wave number decreases and the distance between the instability rolls increases. It follows from figures 4.4(c) that as the field inclination angle increases the wave speed also increases. The numerical results for a stronger magnetizable fluid with the value of $\widetilde{\chi} = \widetilde{\chi}_* = 5$

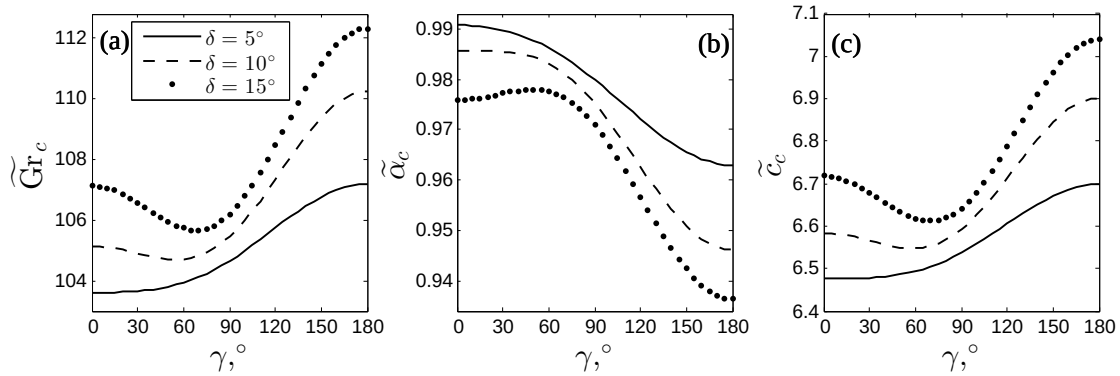

Figure 4.4: Comparison among the critical parameter values: (a) Grashof number $\widetilde{\mathrm{Gr}}$ (the flow is stable under the respective curves), (b) wave number $\widetilde{\alpha}$ and (c) wave speeds $\widetilde{c}$ as functions of the field inclination angles δ and γ for $\widetilde{\mathrm{Gr}}_m = 12$, $H^e = 100$, $\widetilde{\mathrm{Pr}} = 27.5$ and $\widetilde{\chi} = \widetilde{\chi}_* = 3$.

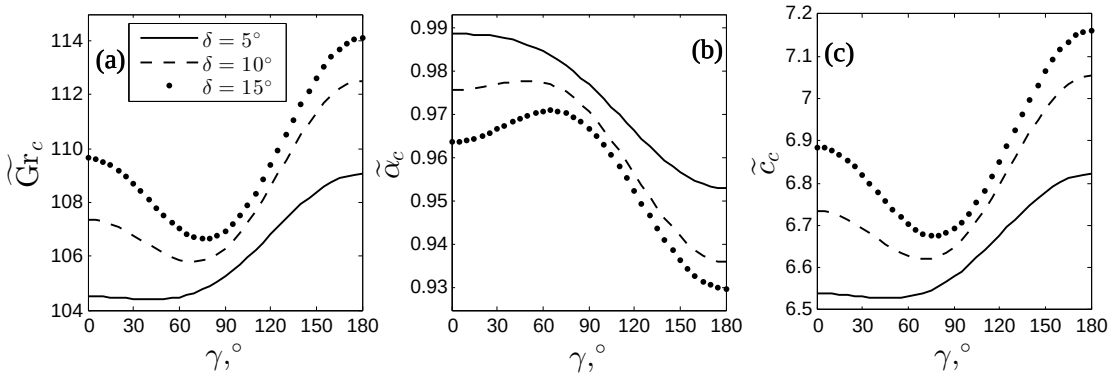

Figure 4.5: Same as figure 4.4 but for $\widetilde{\chi} = \widetilde{\chi}_* = 5$.

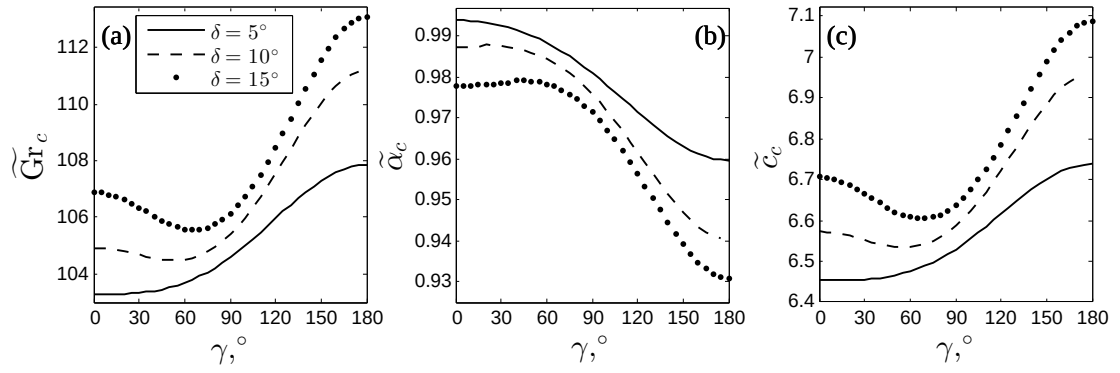

Figure 4.6: Same as figure 4.4 but for $\widetilde{\chi} = 1.5$ and $\widetilde{\chi}_* = 2.5$.

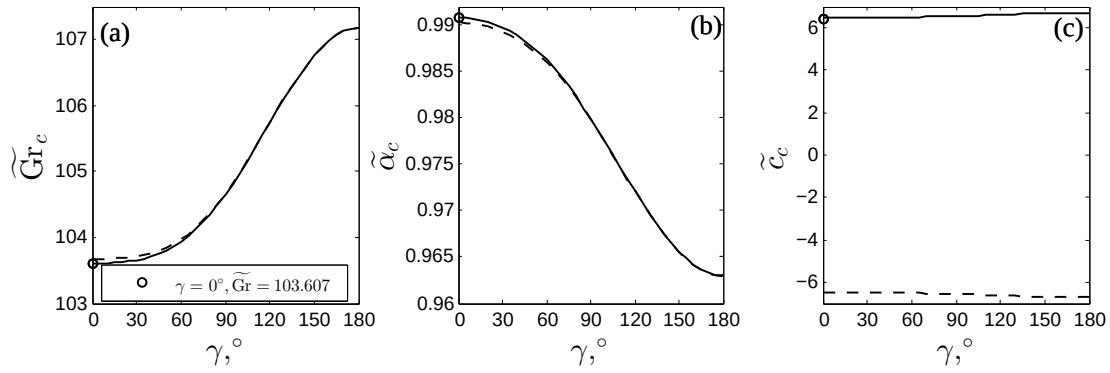

Figure 4.7: Comparison of the critical parameter values for the first (solid line) and second (dashed line) waves: (a) Grashof number $\widetilde{\mathrm{Gr}}$ (the flow is stable under the respective curves), (b) wave number $\widetilde{\alpha}$ and (c) wave speeds $\widetilde{c}$ as functions of the azimuthal angle γ for $\widetilde{\mathrm{Gr}}_m = 12$, $H^e = 100$, $\widetilde{\mathrm{Pr}} = 27.5$, $\delta = 5°$ and $\widetilde{\chi} = \widetilde{\chi}_* = 3$.

are presented in the figure 4.5. It is noticed that, generally the basic flow becomes more stable for stronger magnetizable fluid compared to the weaker magnetizable fluid in the inclined magnetic field at any arbitrary angles. The wave speed propagates faster where as the wave number becomes smaller with the increase the strength of magnetic field in the case of linear magnetization law. In figure 4.6 the critical values of the parameters for the case of non-linear magnetization law closer to magnetic saturation i.e., for $\widetilde{\chi} \neq \widetilde{\chi}_*$ is presented. The comparison with the figures 4.4 and 4.5 does not allow one to make general comment on the flow stability but indicates that the stability parameters have dependencies on a particular combination of the values of δ, γ, χ and χ_*.

The comparison of all three Figures 4.4, 4.5 and 4.6 indicates that stability of the basic flow is influenced more by the value of the differential magnetic susceptibility χ compared to the value of the integral susceptibility χ_*, and generally the basic flow becomes more stable for stronger magnetizable fluids and it's instabilities patterns are characterised by smaller wave numbers and quicker wave speeds compared to weaker magnetizable fluids for all magnetic fields inclination and orientation angles.

As follows the figures 4.7, 4.8 and 4.9 the comparison the critical parameter values of $\widetilde{\mathrm{Gr}}$, $\widetilde{\alpha}$ and $\widetilde{c}$ for the upward and downward waves as function of the azimuthal angle γ from 0 to 180° is presented for $\widetilde{\mathrm{Gr}}_m = 12$, $H^e = 100$, $\widetilde{\mathrm{Pr}} = 27.5$, $\delta = 5°$ and the values $\widetilde{\chi} = \widetilde{\chi}_* = 3$, $\widetilde{\chi} = \widetilde{\chi}_* = 5$ and $\widetilde{\chi} = 1.5$, $\widetilde{\chi}_* = 2.5$ respectively.

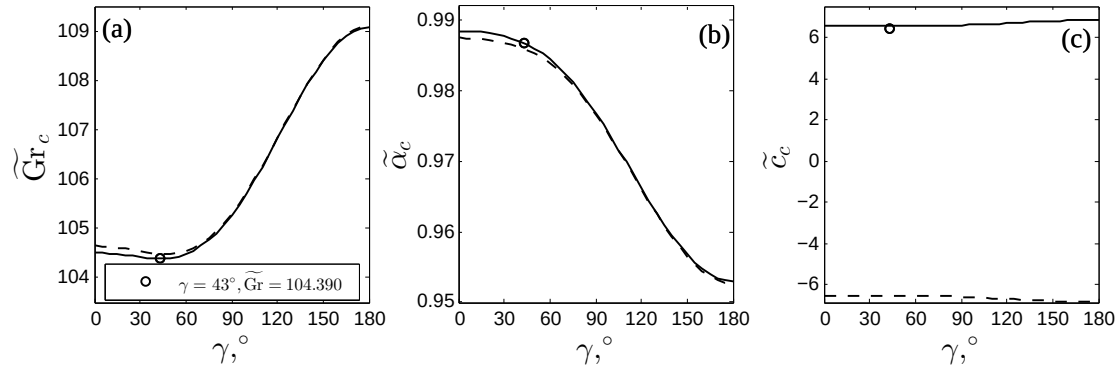

Figure 4.8: Same as figure 4.7 but for $\widetilde{\chi} = \widetilde{\chi}_* = 5$.

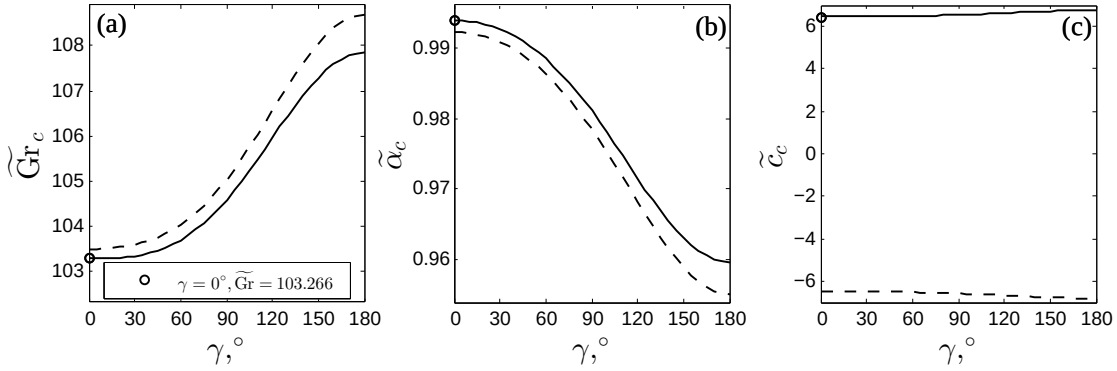

Figure 4.9: Same as figure 4.7 but for $\widetilde{\chi} = 1.5$ and $\widetilde{\chi}_* = 2.5$.

The critical parameter curves for both waves have qualitatively similar forms when the fluid's magnetization law is linear regardless of the degree of fluid magnetization. The results are compared for $\chi = 3$ and $\chi = 5$ shown in figures 4.7, 4.8 respectively. For the two waves the differences between the critical parameters quantitatively are likely same for $\gamma < 90^\circ$ that is when magnetic field lines cross the fluid layer from hot to cold wall upward. For such a field orientation the wavelength of the upward propagating waves becomes slightly shorter than that of the downward waves. The basic flow becomes unstable for $\gamma > 90^\circ$ of both waves almost at the same values of the parameters. The main quantitative difference between the results obtained for $\chi = 3$ and $\chi = 5$ is in the values of the optimal field orientation angle $\gamma_{\min}$. In case of a weaker magnetizable fluid with $\chi = 3$ the orientation angle nearly 0° while for $\chi = 5$ the orientation angle close to 43°. The strength of magnetic effects increases when the optimal field orientation angle approaches 90°. In case of non-linear fluid's magnetization law the main qualitative observation is

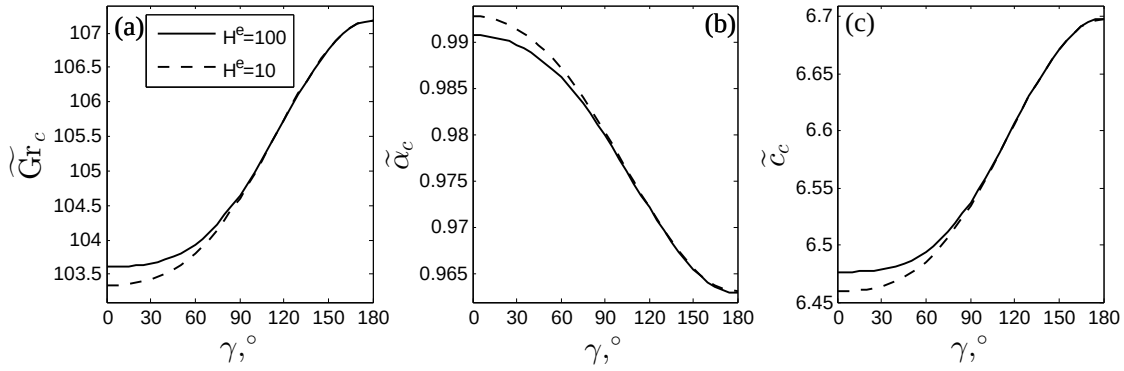

Figure 4.10: Comparison of the critical parameter values for thermo-magnetically less ($H^e = 100$, solid line) and more ($H^e = 10$, dashed line) sensitive fluids: (a) Grashof number $\widetilde{\mathrm{Gr}}$ (the flow is stable under the respective curves), (b) wave number $\widetilde{\alpha}$ and (c) wave speeds $\widetilde{c}$ as functions of the azimuthal angle γ for $\widetilde{\mathrm{Gr}}_m = 12$, $\widetilde{\mathrm{Pr}} = 27.5$, $\delta = 5^\circ$ and $\widetilde{\chi} = \widetilde{\chi}_* = 3$. Type-I instability.

that the critical values of the two waves are clearly distinguishable irrespective of the value of the field orientation angle. Thus in regimes near the fluid magnetic saturation the degree of the up-down symmetry breaking increases.

The stability characteristics of the basic flow with respect to the wave-like disturbances for thermo-magnetically less ($H^e = 100$) and more ($H^e = 10$) sensitive fluids are compared in figures 4.10, 4.11 and 4.12 respectively. The critical parameters for only the upward propagating waves are presented in these figures. It is seen that, the thermo-magnetically less sensitive fluids are more stable than those of there more sensitive counterparts. The distinction in the critical values of magnetic Grashof number, wave number and wave speed are more noticeable for the field orientation angles about 0° to 90° with the regardless of linear magnetization law.

It is also seen that, the wave-like instability patterns arising in a more thermo-magnetically sensitive fluid are characterised by a larger wavenumber and thus by convection structures that are closer packed in the direction of gravity. Furthermore, instability waves arising in a thermo-magnetically less sensitive fluid have a somewhat greater wave speed.

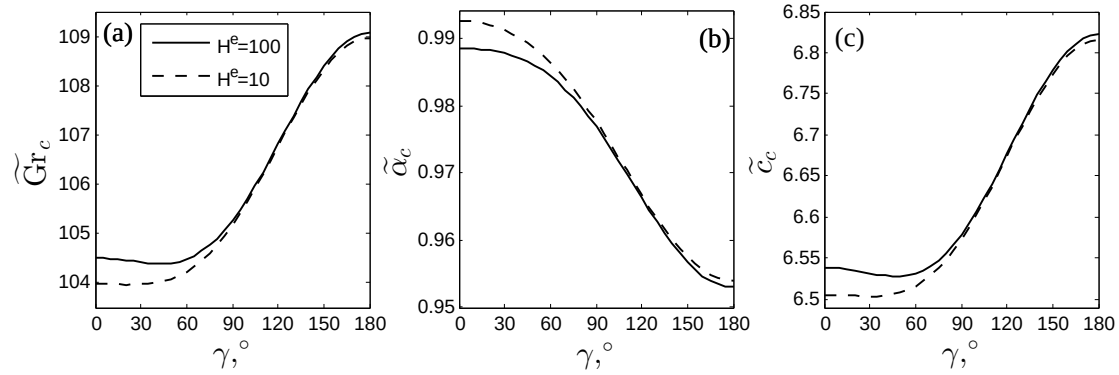

Figure 4.11: Same as figure 4.10 but for $\widetilde{\chi} = \widetilde{\chi}_* = 5$.

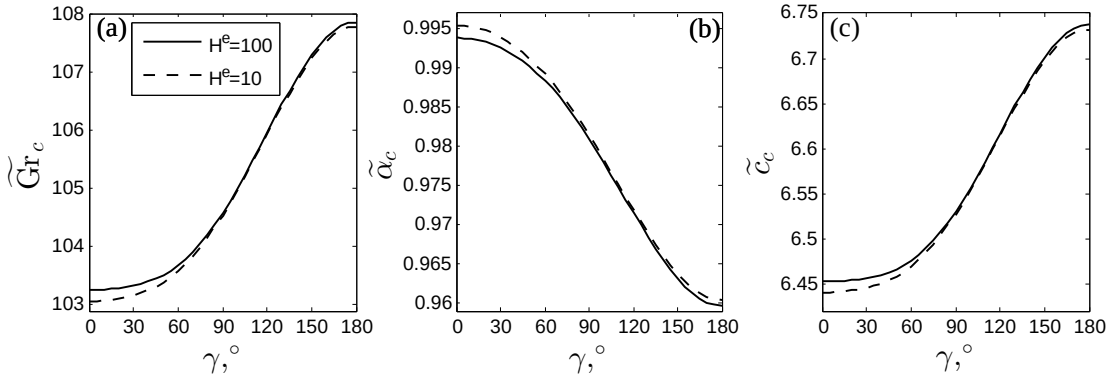

Figure 4.12: Same as figure 4.10 but for $\widetilde{\chi} = 1.5$ and $\widetilde{\chi}_* = 2.5$.

4.2.3 Stability Diagrams

In this section the parametric regions where the different physical mechanisms lead to the threshold of instability in the considered problem geometry will be identified and discussed. To described the physical phenomenon the stability diagrams for an equivalent two-dimensional problem are analyzed here.

Flow instabilities those arise for different values of $\widetilde{\mathrm{Gr}}_c$ with respect to $\widetilde{\mathrm{Gr}}_{mc}$ and corresponding wave number and wave speed are presented in Figure 4.13 where the values of $H^e = 100$, $\widetilde{\mathrm{Pr}} = 27.5$, $\widetilde{\gamma} = 0^\circ$, $\widetilde{\chi} = \widetilde{\chi}_* = 5$ have been considered in a normal magnetic field. This stability diagram has three branches representing the three type of instabilities. The solid line in plot (a) in Figure 4.13 represents the instability of Type-I(solid line) starting at $\widetilde{\mathrm{Gr}}_{mc} = 0$ and $\widetilde{\mathrm{Gr}}_c$ is approximately 108 which is different from the finding of Rahman & Suslov (2016) as there considered $\widetilde{\mathrm{Pr}} = 55$. The corresponding wave numbers

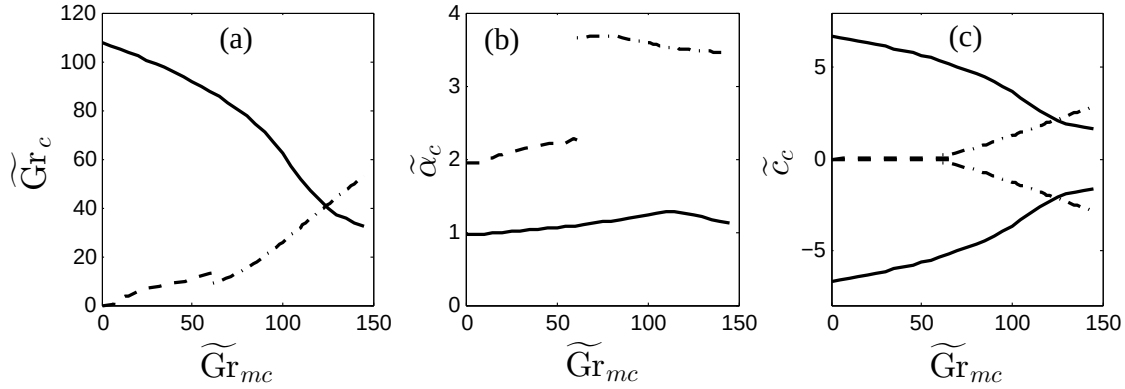

Figure 4.13: (a) Stability diagram for an equivalent two-dimensional problem; (b) the critical wave number $\widetilde{\alpha}_c$ and (c) the corresponding wave speeds along the stability boundaries shown in plot (a) for $H^e = 100$, $\widetilde{\mathrm{Pr}} = 27.5$ and $\widetilde{\chi} = \widetilde{\chi}_* = 5$ in a normal magnetic field ($\delta = 0^\circ$).

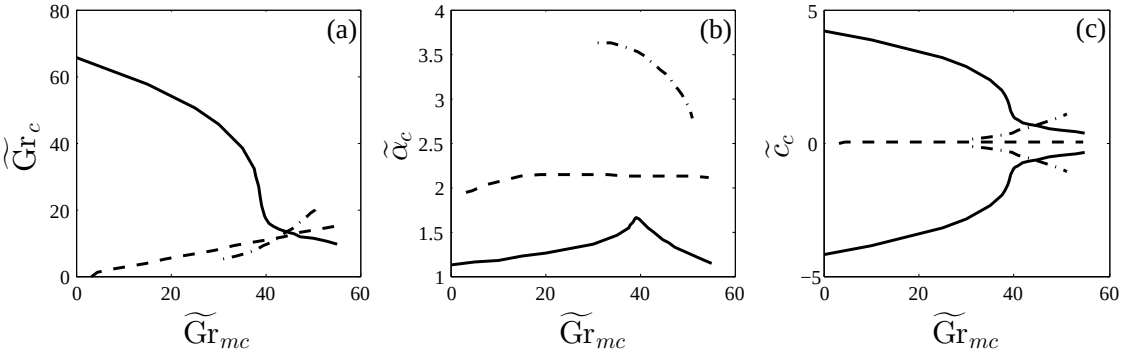

Figure 4.14: (a) Stability diagram for an equivalent two-dimensional problem; (b) the critical wave number $\widetilde{\alpha}_c$ and (c) the corresponding wave speeds along the stability boundaries shown in plot (a) for $H^e = 100$, $\widetilde{\mathrm{Pr}} = 55$ and $\widetilde{\chi} = \widetilde{\chi}_* = 5$ in a normal magnetic field ($\delta = 0^\circ$) [Figure 12, Rahman & Suslov (2016)].

are presented in plot (b) and wave speed in plot (c) in Figure 4.13. From plot (c) it is clear that there are two counterpropagating waves. The instability of Type-II identified by the dashed line starts from $\widetilde{\mathrm{Gr}}_c = 0$. The Type-III instability identified by dash dotted line shown in this figure. It is clear that Type-I instability occurs for low wave number, Type-II instability occurs at moderate wave number and Type-III instability arises for higher wave number. The obtained plots in Figure 4.13 are qualitatively similar to those in Figure 12 (where $\delta = 0^\circ$) in Rahman & Suslov (2016) but quantitatively difference as different $\widetilde{\mathrm{Pr}}$. The stability diagram in plot (a) in Figure 4.13 confirms that fluid convection flow is stable under the solid line and above the dash and dash dotted lines.

The figures 4.15 and 4.16 plotted for the same parameter values as figure 4.13 but with

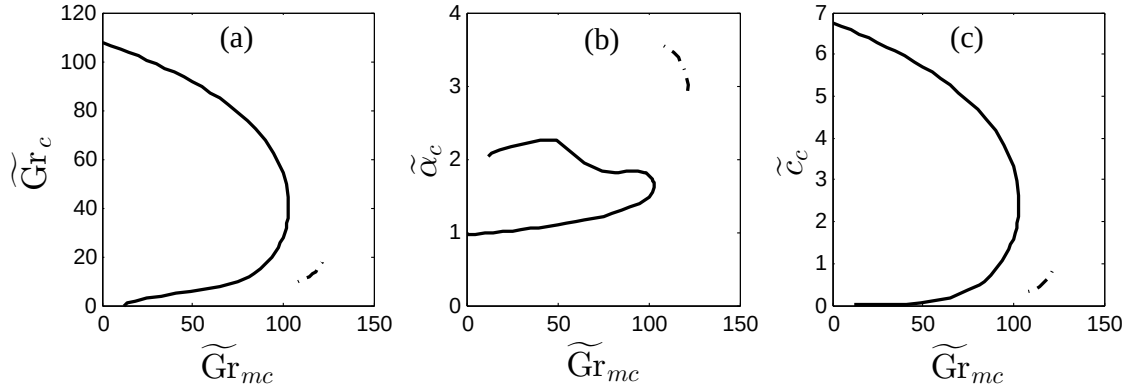

Figure 4.15: (a) Stability diagram for an equivalent two-dimensional problem; (b) the critical wave number $\widetilde{\alpha}_c$ and (c) the corresponding wave speeds along the stability boundaries shown in plot (a) for $H^e = 100$, $\widetilde{\mathrm{Pr}} = 27.5$ and $\widetilde{\chi} = \widetilde{\chi}_* = 5$ in an inclined magnetic field for $\delta = 5^\circ$ and $\widetilde{\gamma} = 0^\circ$.

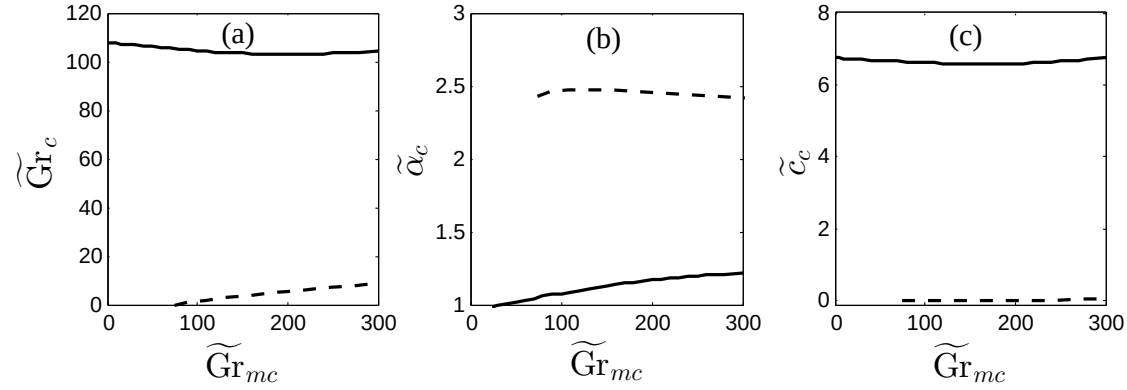

Figure 4.16: (a) Stability diagram for an equivalent two-dimensional problem; (b) the critical wave number $\widetilde{\alpha}_c$ and (c) the corresponding wave speeds along the stability boundaries shown in plot (a) for $H^e = 100$, $\widetilde{\mathrm{Pr}} = 27.5$ and $\widetilde{\chi} = \widetilde{\chi}_* = 5$ in an inclined magnetic field for $\delta = 10^\circ$ and $\widetilde{\gamma} = 0^\circ$.

different values of δ. The stability diagrams in inclined magnetic fields for $\delta = 5^\circ$ and $\delta = 10^\circ$ are shown in figures 4.15 and 4.16 respectively. Here again resemblance are found to this figure 12 (where $\delta = 5^\circ$ and $\delta = 10^\circ$) shown in Rahman & Suslov (2016) qualitatively but quantitatively they are different. It is clear from the diagrams show in figures 4.13, 4.15, 4.16 that the magnetic inclination angle plays significant role in instability characteristics in the flow domain. The solid and dashed stability boundaries shown in Figures 4.13 and 4.15 were distinguishable in Figure 4.13 but merged in case of Figure 4.15 i.e.,the distinction between Type-I and Type-II instabilities blurred when the magnetic field is inclined in a small angle to the vertical plane and Type-III instability is hardly detected with the increase of the field inclination angle. With the further increase

of the field inclination angle the solid line and dashed line are separated completely. The feature matches with the observation reported in Rahman and Suslov(2016). Thus, it can be noted that a change in the Prandtl number has affected the flow stabilization.

Overall discussion about this thesis, it is clearly noted that the basic flow becomes more stable and wave propagates more quicker in lower Prandtl number of fluids compared to the higher Prandtl number of fluids reported in Rahman & Suslov (2016). However, the propagating wave is characterized by smaller wave number in lower Prandtl number of fluids compared to those in higher Prandtl number of fluids.

Chapter 5

Conclusions

The thermomagnetic convection in a vertical layer of ferromagnetic fluid under inclined magnetic field has been analyzed and compared to that reported in Rahman & Suslov (2016). For the analysis purpose the considered fluid has the Prandtl number $\mathrm{Pr} = 27.5$. Both the normal and inclined(at different angles) magnetic fields have been considered to verify it's effect to the previous results. The stability characteristics of basic flow for thermo-magnetically less($H^e = 100$) and more($H^e = 10$) sensitive fluids are investigated. The critical values of thermal Grashof number, wave number and wave speed have been computed for various magnetic susceptibilities. From the result and discussions the following conclusions can be drawn:

(1) For pure gravitational convection the obtained critical values of thermal Grashof number and wave number for different Prandtl number agree with the earlier researches.

(2) At the onset of stationary magneto convection, the wave number is independent of the Prandtl number.

(3) The first(upward propagating) wave remains the most dangerous compared to the second(downward propagating) wave in both (thermo-magnetically more and less sensitive) types of fluids in all regions of flow domain.

(4) With the increasing of the strength of the applied inclined magnetic field, generally, the stability characteristics can change qualitatively.

(5) A comparison between critical parameters (thermal Grashof number, wave number and wave speed) for certain values of other parameters for the considered problem are qualitatively similar to those reported in Rahman & Suslov (2016) but have a quantitatively difference.

(6) A comparison of the obtained stability diagram with those reported in Rahman & Suslov (2016) confirms that the basic flow is more stable with the smaller Prandtl numbers of fluid for both the normal and inclined magnetic field.

References

Abraham, A. (2002), 'Rayleigh-Bénard convection in a micropolar ferromagnetic fluid', *Int. J. Eng. Sci.* **40**, 449–460.

Albrecht, T., Bhrer, C., Fhnle, M., Maier, K., Platzek, D. & Reske, J. (1997), 'First observation of ferromagnetism and ferromagnetic domains in a liquid metal', *Appl. Phys. A-Mater* **65(2)**, 215–220.

Bashtovoy, V. G. Berkovsky, B. M. & Vislovich, A. N. (1988), *Introduction to thermomechanics of magnetic fluids*, Hemisphere, Washington, DC.

Belyaev, A. V. & Smorodin, B. L. (2010), 'The stability of ferrofluid flow in a vertical layer subject to lateral heating and horizontal magnetic field', *J. Magn. Magn. Mater.* **322**, 2596–2606.

Berkovskii, B. M. & Bashtovoi, V. G. (1971), 'Gravitational convection in a ferromagnetic liquid', *Magnitnaya Gidrodinamika* **7**, 24–28.

Blums, E., Cebers, A. O. & Maiorov, M. M. (1997), *Magnetic Fluids*, Walter de Gruyter.

Blums, E. Y., Maiorov, M. M. & Tsebers, A. O. (1989), *Magnetic Fluids*, Zinatne, Riga, Latvia (in Russian).

Bogatyrev, G. P. & Gilev, V. G. (1984), 'Concentration dependence of the viscosity of a magnetic liquid in an external field', *Magnetohydrodynamics* **20**, 249–252.

Bozhko, A. A., Putin, G. F., Sidorov, A. S. & Suslov, S. A. (2013), 'Convection in a vertical layer of stratified magnetic fluid', *Magnetohydrodynamics* **49**, 143–152.

Elmore, W. C. (1938), 'The magnetisation of ferromagnetic colloids', *Phys. Rev.* **54**, 1092–1095.

Finlayson, B. A. (1970), 'Convective instability of ferromagnetic fluids', *J. Fluid Mech.* **40**, 753–767.

Gershuni, G. Z., Zhukhovitsky, E. M. & Nepomniaschy, A. A. (1989), *Stability of Convective Flows*, Science, Moscow, Russia (in Russian).

Huang, J., Edwards, B. F. & Gray, D. D. (1997), 'Thermoconvective instability of paramagnetic fluids in a uniform magnetic field', *Phys. Fluids* **9(6)**, 1819–1825.

Lange, A., Reiman, B. & Richter, R. (2000), 'Wave number of maximal growth in viscous magnetic fluids of arbitrary depth', *Phys. Rev. E* **61**, 5528–5539.

Odenbach, S. (2002), *Ferrofluids: magnetically controllable fluids and their applications*, Springer, New York.

Rahman, H. & Suslov, S. A. (2015), 'Thermomagnetic convection in a layer of ferrofluid placed in a uniform oblique external magnetic fluid', *J. Fluid Mech.* **764**, 316–348.

Rahman, H. & Suslov, S. A. (2016), 'Magneto-gravitational convection in a vertical layer of ferrofluid in a uniform oblique magnetic fluid', *J. Fluid Mech.* **795**, 847–875.

Rosensweig, R. E. (1979), 'Fluid dynamics and science of magnetic fluids', *Adv. Electron El. Phys.* **48**, 103–199.

Rosensweig, R. E. (1985), *Ferrohydrodynamics*, Cambridge University Press.

Russell, C. L., Blennerhassett, P. J. & Stiles, P. J. (1995), 'Large wave number convection in magnetized ferrofluids', *J. Magn. Magn. Mater.* **149**, 119–121.

Russell, C. L., Blennerhassett, P. J. & Stiles, P. J. (1999), 'Supercritical analysis of strongly nonlinear vortices in magnetized ferrofluids', *Proc. R. Soc. Lond.* **455**, 23–67.

Schwab, L., Hildebrandt, U. & Stierstadt, K. (1983), 'Magnetic Bénard convection', *J. Magn. Magn. Mater.* **39**, 113–114.

Shliomis, M. I. & Smorodin, B. L. (2002), 'Convective instability of magnetized ferrofluids', *J. Magn. Magn. Mater.* **252**, 197–202.

Siddheshwar, P. G. (1993), 'Rayleigh-Bénard convection in a ferromagnetic fluid with second sound', *Jpn. Soc. Mag. Fluids* **25**, 32–36.

Siddheshwar, P. G. (1995), 'Convective instability of ferromagnetic fluids bounded by fluid-permeable, magnetic boundaries', *J. Magn. Magn. Mater.* **149**, 148–150.

Suslov, S. A. (2008), 'Thermo-magnetic convection in a vertical layer of ferromagnetic fluid', *Phys. Fluids* **20(8)**, 084101.

Suslov, S. A., Bozhko, A. A. & Putin, G. F. (2008), Thermo-magneto-convective instabilities in a vertical layer of ferro-magnetic fluid, *in* 'Proceedings of the XXXVI International Summer School—Conference "Advanced Problems in Mechanics"', Repino, Russia, pp. 644–651.

Suslov, S. A., Bozhko, A. A., Putin, G. F. & Sidorov, A. S. (2010), 'Interaction of gravitational and magnetic mechanisms of convection in a vertical layer of a magnetic fluid', *Physics Procedia* **9**, 167–170.

Suslov, S. A., Bozhko, A. A., Sidorov, A. S. & Putin, G. F. (2012), 'Thermomagnetic convective flows in a vertical layer of ferrocolloid: Perturbation energy analysis and experimental study', *Phys. Rev. E* **86**, 016301.

Suslov, S. A. & Paolucci, S. (1995), 'Stability of natural convection flow in a tall vertical enclosure under non-Boussinesq conditions', *Int. J. Heat Mass Transfer* **38**, 2143–2157.

Tynjälä, T. (2005), Theoretical and numerical study of thermomagnetic convection in magnetic fluids, PhD thesis, Lappeenranta University of Technology, Lappeenranta, Finland.

Vaidyanathan, G., Sekar, R. & Balasubramanian, R. (1991), 'Ferroconvective instability of fluids saturating a porous medium', *Int. J. Eng. Sci.* **29**, 1259–1267.